RSC Sustainability

Accepted Manuscript

RSC Sustainability

ROYAL SOCIETY OF CHEMISTRY

ROYAL SOCIETY OF CHEMISTRY

Sustainability spotlight

In the past few decades, the chemistry of bromine radicals has been well studied, and especially transition-metal-based and heat-assisted radical-based strategies have been well developed. Furthermore, recent advancements in the field of radical chemistry have enabled chemists to explore direct functionalization *via* HAT. Unfortunately, these previous strategies require expensive metals and ligands, high temperatures, and toxic radical initiators, thus, making them unsustainable. The development of simple and mild methodologies for bromine radical-enhanced hydrogen atom transfer reaction for the formation of C-centered radical intermediates under visible light is highly desirable. Visible light as an energy source for the reaction reduces the need for harmful UV light and aligns with green sustainable principles for the formation of C-C and C-X bond formation via bromine-assisted HAT. Moreover, the developed photocatalytic systems enhance the reaction efficiency and selectivity making it more sustainable. Photocatalysts like transition metal complexes or organic dyes can activate bromine under visible light irradiation, facilitating the HAT process, which further facilitates C-C and C-X bond formation. Our review emphasizes the importance of the following UN sustainable development goals: affordable and clean energy (SDG 7), industry, innovation, and infrastructure (SDG 9), chemical and waste.

RSC Sustainability Accepted Manuscript

No primary research results, software or code have been included and no new data were generated or analysed as part of this review.

ARTICLE

Visible Light-Induced Bromine Radical Enhanced Hydrogen Atom Transfer (HAT) Reactions in Organic Synthesis

Barakha Saxena,[a] Roshan I. Patel,[a] and Anuj Sharma*[a]

Hydrogen atom transfer (HAT) reactions have gained a prominent space in organic synthesis for allowing a straightforward approach towards C-H bond activation for the formation of C-centered radical intermediates. However, halogen radical-assisted hydrogen atom transfer (HAT) reactions have become an interesting tool toward C-H bond activation, allowing for the formation of C-C and C-X bond formations. In particular, the bromine radical (Br$^\bullet$) has garnered attention for its remarkable capability as a hydrogen acceptor, which abstracts an H-atom from a C-H bond and generates a C-centered radical intermediate. Typically, transition metal- and organo-photocatalysts are commonly used to generate bromine radical (Br$^\bullet$) from bromine anion (Br$^-$). This newly generated bromine radical (Br$^\bullet$) is useful in several organic transformations *via* C-H bond activation. Hereby, in this review, we provide recent updates on bromine radical (Br$^\bullet$) assisted hydrogen atom transfer (HAT) reactions with their scope, mechanism, and limitations.

1. Introduction

In synthetic organic chemistry, photocatalysis has undergone significant growth providing a wide range of useful transformations for accessing valuable organic compounds.[1] Typical photoredox catalysts such as metal photocatalysts (Ru- and Ir- complexes) and organic dyes (Eosin Y, Rose Bengal acridinium-based, etc.) have served as popular photocatalysts by harnessing the oxidative/reductive capabilities of both organo-photocatalysts and transition metal (TM) photocatalysts in their activated state. These catalysts efficiently facilitate a broad range of reactions through single electron transfer (SET) or energy transfer (EnT) mechanisms due to their long-excited state lifetimes and useful photoredox potential.[2] Moreover, substrates or additives capable of forming electron-donor acceptor (EDA) complexes in the ground state have also come under the light as an efficient method for C-C and C-X bond formation.[3] In this regard, a new platform has recently emerged that combines photoredox catalysis with halide ion catalysis. They are coordinatively saturated and stable avoiding any ligand exchange with reaction partners.[4] The proposed mechanism is based on a single electron transfer (SET) from the photo-excited catalyst to the halide ion (X$^-$) to generate a halide radical (X$^\bullet$) that promotes HAT from a substrate C-H bond. A hydrogen atom transfer (HAT) reaction involves the transfer of a hydrogen atom from a hydrogen donor (C-H) to a hydrogen acceptor (X$^\bullet$) and has attracted considerable
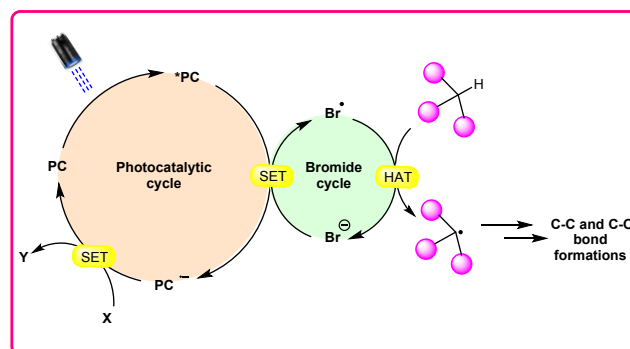
Scheme 1. General approach toward the generation of bromine radical and hydrogen atom transfer process.

attention due to its capability for functionalizing complex molecules *via* C-H bond activation.[5] HAT reactions are particularly relevant in the context of radical chemistry, where a radical species (X$^\bullet$) abstracts a hydrogen atom from another molecule, resulting in the formation of a new radical and a different compound. The driving force behind HAT reactions is typically the difference in the stability of the radical intermediates formed before and after the transfer. This process is important in various chemical reactions, including those involved in organic, inorganic, and biological systems.

Consequently, the utilization of a radical reagent capable of forming bonds that are more stable than those to be cleaved can enable direct functionalization *via* HAT. Various radical species (X$^\bullet$), such as O-, N-, S-, B-, and halogen-centered radicals, have been identified as suitable HAT reagents.[6] Among these, halogen radicals have garnered significant interest due to their ease of accessibility and high reactivity.

[a.] Department of Chemistry, Indian Institute of Technology Roorkee, Roorkee-247667, India.
E-mail: : anujsfcy@iitr.ac.in, anujsharma.mcl@gmail.com ;
Tel: +91-1332-284751
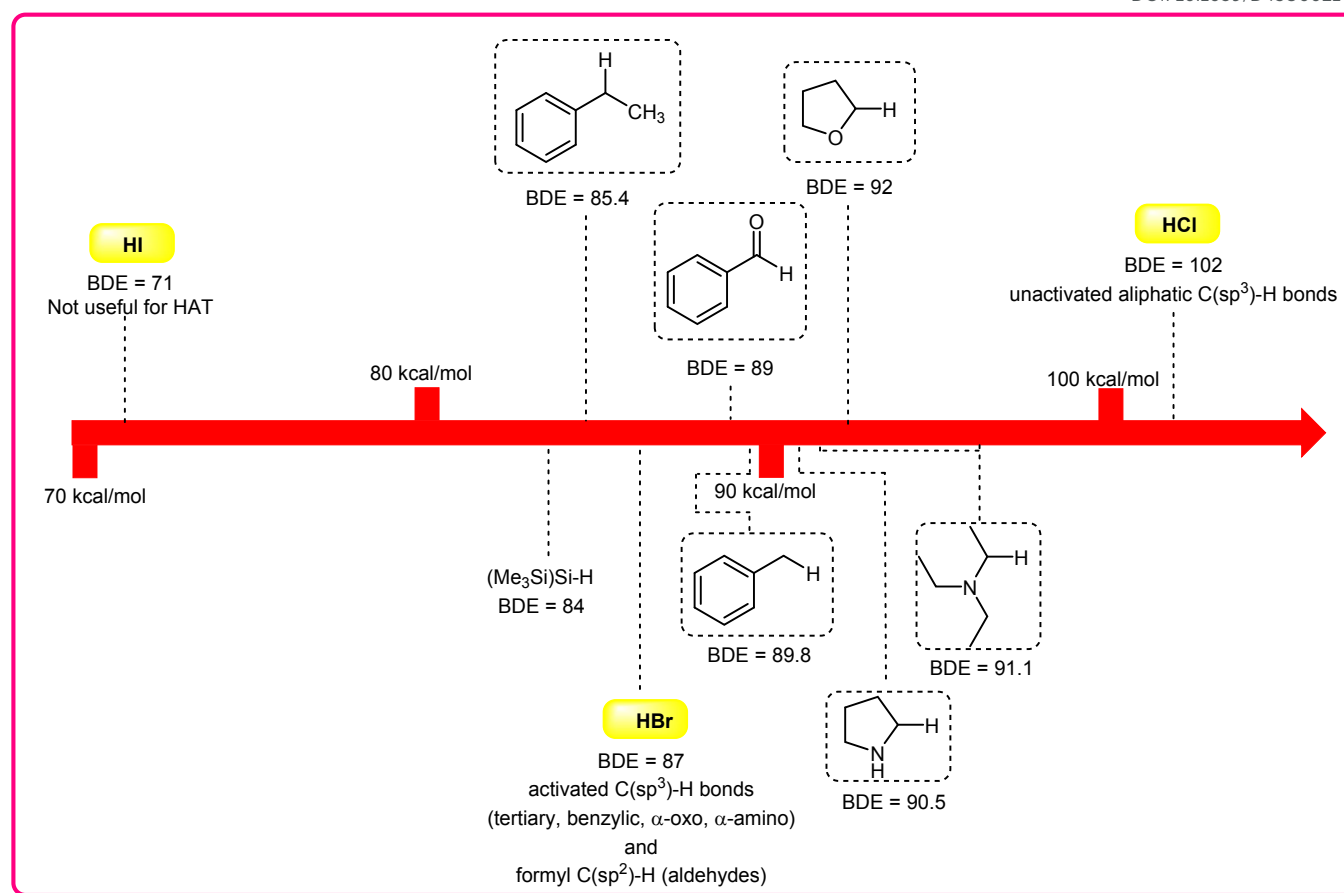
Scheme 2. Bond dissociation energies (kcal/mol) of C–H bonds and those of H–X bond

Halogen radicals, especially chlorine radical (Cl•) and bromine radical (Br•), serve as a potent hydrogen acceptor and play a crucial role as agents for facilitating hydrogen atom transfer (HAT).[7] Bromine radical (Br•) is a highly reactive species with an unpaired electron, which makes it capable of abstracting a hydrogen atom from a nearby molecule, leaving behind hydrogen bromide (HBr). The X–H (X= C, Si) bond dissociation energies (BDEs) of the hydrocarbons listed in Scheme 2 are generally in the vicinity of the bond formation energy of H–Br (87 kcal mol^{-1}).[8] Therefore, bromine radical (Br•) demonstrates a facile ability to cleave the X–H (X= C, Si) bonds. Conversely, iodine radicals (I•) exhibit minimal to no capability for engaging in C-H bond activation.[8b] There have been significant efforts devoted to C-H bond activations *via* hydrogen atom transfer (HAT), which can be seen in a few excellent review articles.[9] Some of the notable ones are by Ravelli and co-workers in 2020, who discuss the direct, indirect, and remote photocatalytic HAT reactions for the formation of C-centered radical intermediate.[9a] However, photocatalytic hydrogen atom transfer (HAT), where halogen radicals are involved in the activation of the C-H bonds was not discussed by them. Next, in 2022, Capaldo and co-workers, nicely penned an article on photocatalytic halogen-radical assisted HAT reactions, however, HAT reactions *via* bromine radical were merely covered.[10] Later, in 2023, Itabashi, Asahara, and Ohkubo, presented an excellent review on the chloride radical (Cl•)-mediated C-H oxygenation strategies *via* HAT for the formation of the C-O bond.[11]

As per our knowledge, there has been no review article exclusively focused on visible light-mediated hydrogen atom transfer (HAT) reactions using bromine radical (Br•). Within this framework the present article is written, addressing strategies involving bromine radical (Br•) mediated hydrogen atom transfer (HAT) under visible light irradiation for the generation of C-C and C-O bonds. The contents of the review are categorized into various types of hydrogen atom transfer reactions from bromine radical (Br•) such as (1) Hydrogen atom transfer from aldehydes (2) Hydrogen atom transfer from benzylic carbons (3) Hydrogen atom transfer from α-hetero carbons (4) Hydrogen atom transfer from (Me$_3$Si)$_3$SiH (5) Hydrogen atom transfer from allylic carbons (6) Miscellaneous

2. Hydrogen atom transfer from aldehydes

Hydrogen atom transfer (HAT) from aldehydes involves the transfer of a hydrogen atom from an aldehyde molecule to another molecule or radical intermediate. The hydrogen atom attached to the carbonyl carbon in aldehydes is relatively acidic due to the electron-withdrawing nature of the carbonyl group. Initially, the HAT reaction is initiated by the generation of a bromine radical (Br•), often through the excited photocatalyst (*PC) *via* reductive quenching. This resulting bromine radical (Br•) abstracts a hydrogen atom bound to the carbon atom adjacent to the carbonyl group. The abstraction
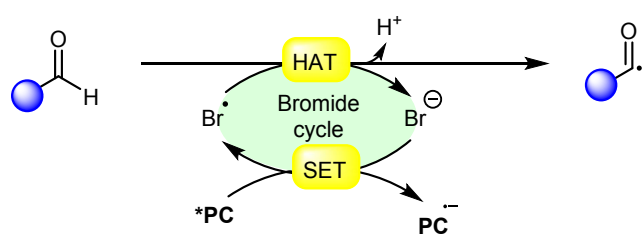
Scheme 3. General approach for acyl radical intermediate formation *via* bromine radical mediated HAT.

occurs due to the high reactivity of the bromine radical species (Br•), which seeks to stabilize itself by pairing its unpaired electron with an electron from the hydrogen atom, thus forming a new covalent bond. Moreover, the abstraction of the hydrogen atom leads to the formation of an acyl radical intermediate, which contains an unpaired electron, making it highly reactive and prone to further chemical reactions. The generation of an acyl radical *via* bromine radical-mediated HAT is shown in Scheme 3.

In 2020, Huang and co-workers published a photoredox Minisci-type alkylation of pyridines **1** with aliphatic and aromatic aldehydes **2** as the umpolung alkylating reagent (Scheme 4).[12] Under the optimized conditions, the authors were able to demonstrate the Minisci-type alkylation of some bioactive molecules such as quinoxyfen and fasudil in 40% and 50% yield respectively. Various mechanistic studies such as H/D exchange, a kinetic isotopic effect (KIE) experiments, and Stern-Volmer quenching studies were performed to understand the reaction mechanism. Mechanistically, the photoexcited catalyst *Ir(III) undergoes a single electron transfer (SET) process with a bromide ion (Br⁻) to generate bromine radical (Br•) and Ir(II). This bromine radical (Br•) would abstract a hydrogen atom from aldehyde **2** *via* deprotonated electron transfer (DPET) to access the acyl radical **4A**. The resulting intermediate **4A** adds to the *N*-heterocycle **1**, accompanied by deprotonation, and subsequent spin-center shift (SCS) occurs to generate the hydroxyalkyl radical intermediate **4D**. Next, the SET process from the reductive Ir(II) to the intermediate **4D** furnishes the intermediate **4E**. Furthermore, the reduction of **4E** with aldehyde **2** affords the final product **3**. With a change in reaction conditions, the authors further demonstrated the benzylation of nitrogen-containing heteroarenes **1** using benzaldehydes **2** by employing 4CzIPN as the photocatalyst, with CF₃SO₃H and (PhO)₂PO₂H as the acid, LiBr as the additive in chlorobenzene (PhCl) under visible light irradiation affording the desired products **3** in 21-83% yield.

Wang, Huang, and co-workers in 2020 illustrated a dual photoredox/bromide catalyzed Minisci hydroxyalkylation of quinolines **4** using aldehydes **2** under visible light irradiation (Scheme 5).[13] Inexpensive LiBr was chosen to be an efficient moderator for this protocol with 4CzIPN as an organo-photocatalyst under visible light irradiation.
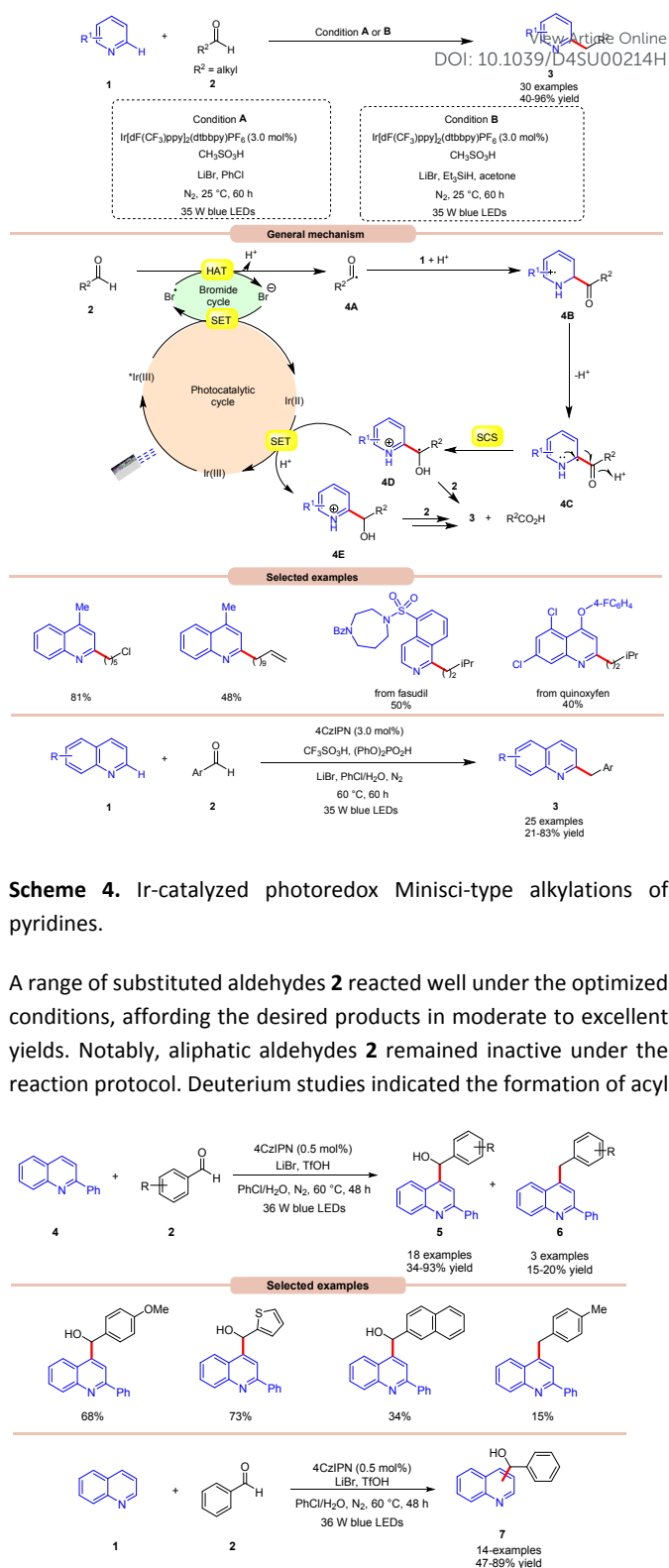
Scheme 4. Ir-catalyzed photoredox Minisci-type alkylations of pyridines.

A range of substituted aldehydes **2** reacted well under the optimized conditions, affording the desired products in moderate to excellent yields. Notably, aliphatic aldehydes **2** remained inactive under the reaction protocol. Deuterium studies indicated the formation of acyl
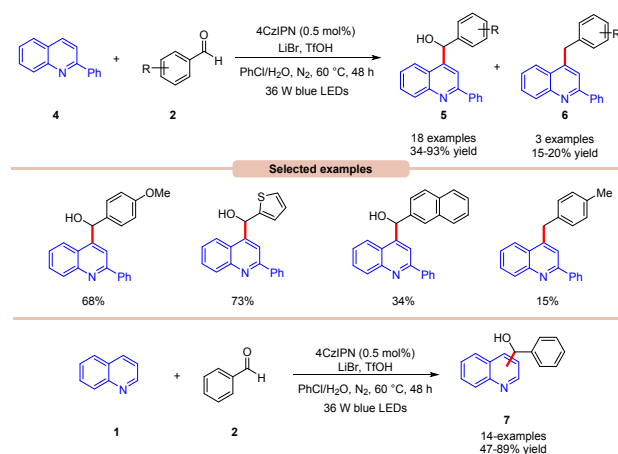
Scheme 5. Dual 4CzIPN/LiBr mediated Minisci hydroxyl alkylation of quinolines with aryl aldehydes.

ARTICLE
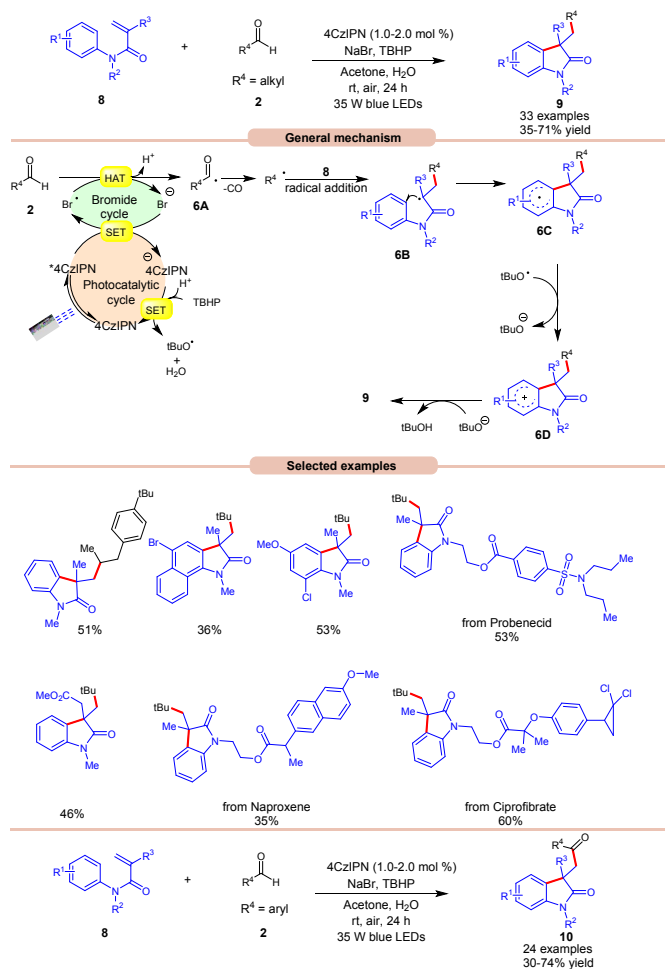
Scheme 6. 4CzIPN-catalyzed radical acylation of *N*-arylacrylamides with aliphatic or aromatic aldehydes.

radical *via* C-H scission of aldehyde **2**, which was further proven by the TEMPO trapping experiment. Stern-Volmer experiment reveals that 4CzIPN could efficiently oxidize the bromide anion, thus forming the bromine radical intermediate. Finally, the light-on-off experiment found the visible light irradiation crucial for the reaction protocol. Based on these findings, the authors proposed that the generated bromine radical intermediate undergoes HAT with the aldehyde **2** to form an acyl radical intermediate which reacts with the quinoline **4**, followed by a similar mechanistic pathway as described in Scheme 4 to give the final product **5**. Under the same reaction condition, a broad range of quinolines **1** was also feasible to yield the desired hydroxyalkylated product **7**. This protocol is limited to quinolines as it fails to undergo a Minisci-type reaction with benzothiazole, benzo-oxazole, and quinoxalinone.

Oxindoles are quintessential moieties in pharmaceuticals, organic materials, and natural products.[14] Great attention has been made for their synthesis. Deng and co-workers in 2022, established a visible light-induced radical alkylation of *N*-arylacrylamides **8** with aliphatic aldehydes **2** (Scheme 6).[15] The authors employed 4CzIPN as a photocatalyst with NaBr as an additive, and TBHP as an oxidant under visible light irradiation. Both electron-donating and electron-withdrawing groups at various positions of the aryl ring of *N*-

arylacrylamides **8** were well tolerated. Moreover, the aliphatic aldehydes **2** containing cyclic and acyclic groups showed good reactivities under the reaction conditions. A key feature of this strategy was illustrated in the late-stage functionalization of naproxen, ibuprofen ciprofibrate, and probenecid drug molecules. Radical trapping experiments with TEMPO, BHT, or 1,1'-diphenylethylene, completely suppressed the reaction, which supported the involvement of a radical mechanistic pathway. Based on these findings and several other controlled experiments, the authors proposed a plausible mechanism, as illustrated in Scheme 6. The photoexcited catalyst 4CzIPN* oxidizes the bromide anion to generate bromine radical *via* a SET process, which participates in HAT with the aldehyde **2** to form acyl radical intermediate **6A**, followed by carbon monoxide (CO) removal to form an alkyl radical intermediate. Next, the alkyl radical adds to the *N*-arylacrylamides **8**, accompanied by cyclization to give access to radical intermediate **6C**. Lastly, SET/deprotonation of **6C** yields the required alkylated product **9**. Furthermore, under similar photocatalytic conditions, the authors demonstrated the acylation of *N*-arylacrylamides **8** using aromatic aldehydes **2** to afford the required acylated products **10**. Notably, replacing aliphatic aldehydes with aromatic aldehydes with the same optimized conditions provides the acyl-substituted oxindoles **10** in 30-74% yields. Probably secondary and tertiary aliphatic aldehyde undergoes decarbonylation due to the formation of stable alkyl radicals.
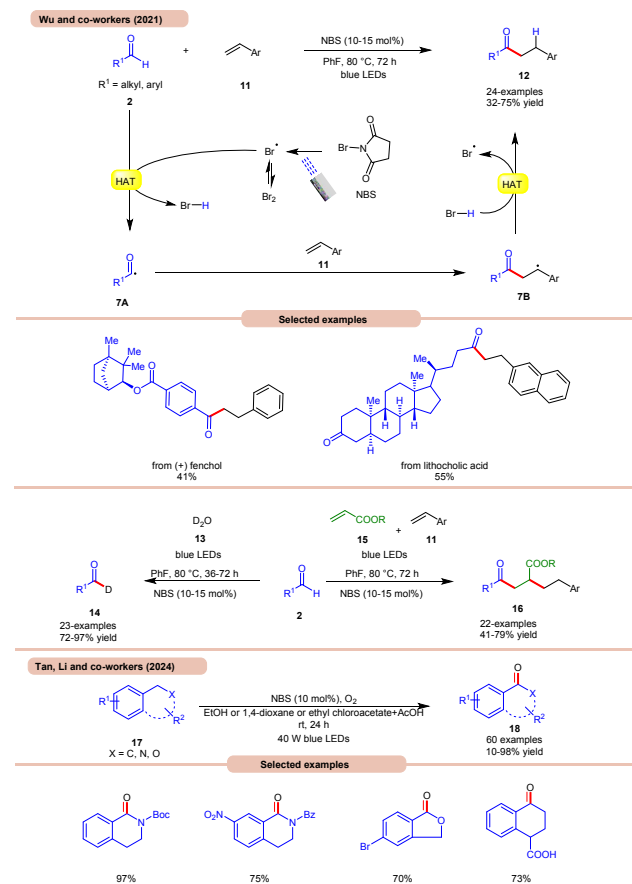

Scheme 7. Bromine-radical catalyzed hydroacylation of vinyl arenes.

Journal Name

ARTICLE

A highly effective approach towards the hydroacylation of vinyl arenes **11** was accomplished by Wu and co-workers using *N*-bromosuccinimide (NBS) as a catalyst under visible light irradiation (Scheme 7a).[16a] The striking feature of this protocol is that it does not require any external photocatalyst to generate the bromine radical. The ideal reaction conditions comprised of NBS in fluorobenzene at 80 °C under blue light irradiation. Notably, the application of a non-aromatic solvent in the reaction mixture failed to give the targeted product. A broad range of styrene derivatives **11** reacted well with alkyl and aryl aldehydes **2** affording the hydroacylated product **12** in 32-75% yield. TEMPO trapping experiment inhibited the product formation, indicating a radical mechanistic pathway. Light on/off studies indicated that visible light irradiation is crucial for the homolysis process. As shown in Scheme 7, in the presence of visible light irradiation, NBS undergoes N-Br bond homolysis to give bromine radical in equilibrium with molecular bromine. Subsequently, the aldehyde group **2** undergoes HAT with the bromine radical to give HBr and acyl radical intermediate **7A**, which adds to the terminal alkene position to give a benzyl radical intermediate **7B**. Lastly, the desired product **12**, is obtained *via* HAT with HBr. Product formation was further supported by DFT calculations. This strategy could also be applicable to the deuteration of aldehydes **2** with D_2O **13** affording the deuterated product **14** in 72-97% yield. The compatibility of this protocol was further seen in the radical cascade reaction involving acrylates **15** and styrene **11** giving the desired product **16** in 41-79% yield.

Most recently, Tan, Li, and co-workers developed a metal-free photocatalytic system for aerobic oxygenation of benzylic C(sp3)-H bonds of amines, ethers, alkylarenes, and hetero-aromatics **17** (Scheme 7b).[16b] In this method, the authors employed readily available NBS as a bromine radical source and O_2 as an oxidant. The method has been successfully applied to the synthesis of bioactive and drug-valued targets including corydaldine, ketoprofen, and isoflavone, providing good opportunities for applications in drug discovery and development.

Impressively, a new methodology for the synthesis of ketones **20** was developed by Kawasaki, Ishida, and Murakami, in 2020 by using a dual Ir-photoredox/nickel catalytic system (Scheme 8).[17] In this strategy, $NiBr_2$(dtbby) plays a dual role in the generation of a bromine radical and in the cross-coupling of benzylic and acyl radical intermediate. A variety of alkylarenes **19** was well tolerated with alkyl aldehydes **2** under the optimized conditions to yield the corresponding ketones **20** in 22-80% yields. TEMPO trapping experiment supported the formation of benzylic and acyl radical intermediate. Mechanistically, an anion exchange interaction between Ir-photoredox and $NiBr_2$(dtbbpy) catalytic system gives [Ir(III)][Br]-complex **8A**, which in the presence of visible light irradiation gives access to bromine radical and Ir(II)-complex **8B** *via* SET event between photoexcited [Ir(III)]* and bromide anion.
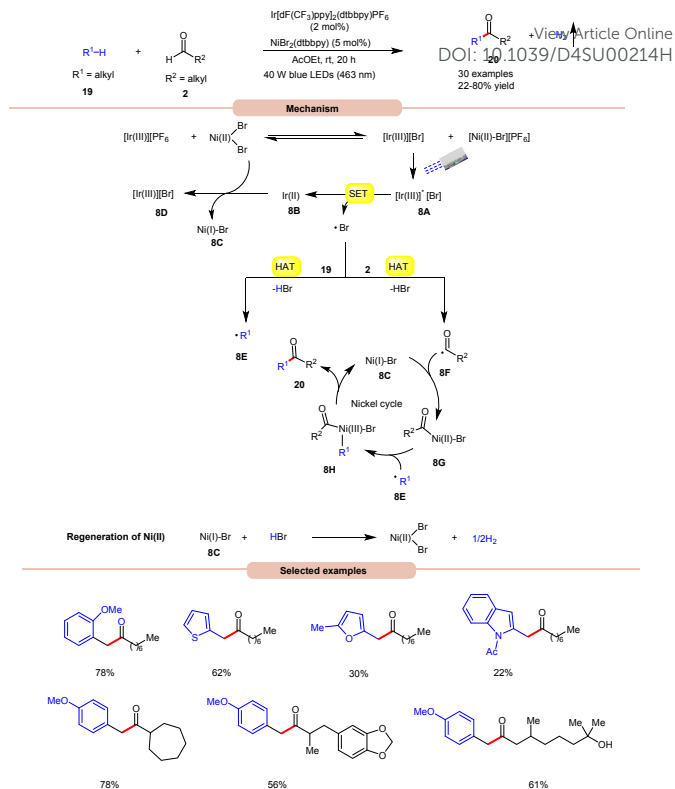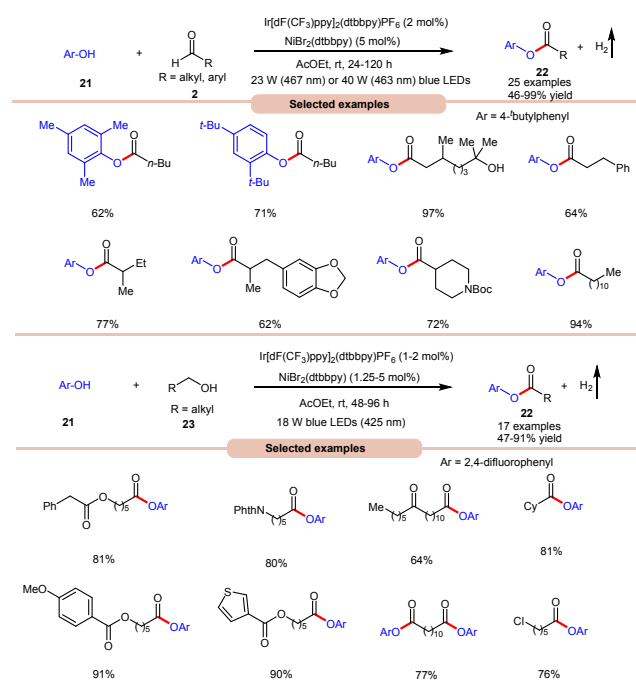

Scheme 8. Bromine radical-mediated dehydrogenative coupling reaction for the synthesis of aryl ketones.

Subsequently, the bromine radical participates in a HAT reaction with the aldehyde **2** and benzylic **19** C-H bond to give acyl radical intermediate **8F** and benzylic radical intermediate **8E** along with HBr. The resulting acyl radical intermediate **8F** interacts with Ni(I)Br-species **8C** to give access to Ni(II)-Br species **8G**. Next, Ni(II)-Br species **8G** interacts with benzylic radical intermediate **8E** to give Ni(III)-Br complex **8H**. Lastly, reductive elimination generates the final product **20** with the regeneration of **8C**. Moreover, the interaction between **8C** and HBr regenerates the corresponding Ni-catalyst along with H_2. Notably, benzaldehydes did not yield successful outcomes in this protocol, primarily due to the challenge in abstracting the aldehydic hydrogen. This difficulty arises from the electron-withdrawing nature of the phenyl group attached to the aldehyde.

With a slight change in the optimized conditions, the same group later reported a visible light-mediated acylation of phenols **21** with aldehydes **2** for the synthesis of esters **22** under a dual Ir-photoredox/nickel bromide catalytic system (Scheme 9a).[18a] A broad range of aromatic phenols **21** and alkyl and aryl aldehydes **2** reacted well to afford the corresponding esters **22** in 46-99% yield. The robustness of this protocol was compatible with naturally occurring phenols such as β-arbutin and α-tocopherol. In continuation of their work, the same group later reported the acylation of phenols **21** using alkyl alcohols **23** to afford the required acylated products **22** in 47-91% yields under similar reaction conditions (Scheme 9b).[18b]

RSC Sustainability Accepted Manuscript

Scheme 9. Bromine radical-mediated acylation of phenol with aldehydes and alcohols.

3. Hydrogen atom transfer from benzylic carbons

Hydrogen atom transfer (HAT) from a benzylic carbon refers to the abstraction of a hydrogen atom bonded to a carbon atom adjacent to a benzene ring. When a bromine radical species interacts with a substrate containing a benzylic carbon, it can abstract a hydrogen atom from this position, leading to the formation of a benzylic radical intermediate. Notably, benzylic hydrogen atoms are more readily abstracted in comparison to other hydrogen atoms in a molecule due to the stability of the resulting benzylic radical, which is resonance-stabilized by the delocalization of the unpaired electron into the aromatic ring.
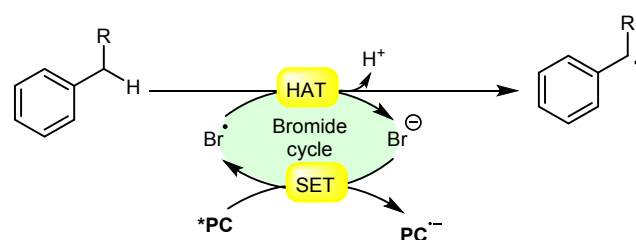

Scheme 10. General approach for benzyl radical intermediate formation *via* bromine radical-mediated HAT.
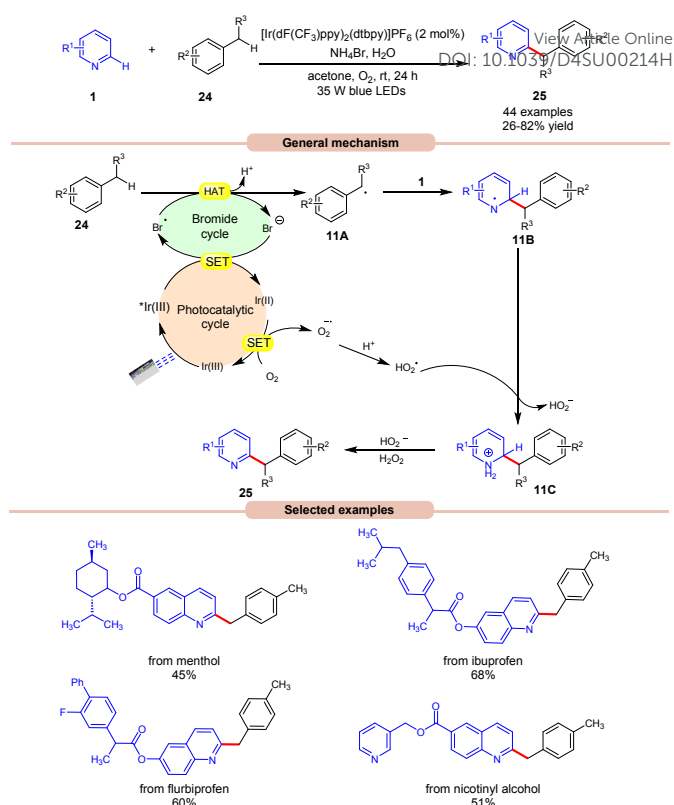
Scheme 11. Dual Ir-photoredox/NH$_4$Br catalyzed cross-dehydrogenative coupling of *N*-heteroarenes with toluenes.

In this regard, an aerobic cross-dehydrogenative coupling (CDC) reaction was achieved by Huang, Deng, and co-workers in 2021 by the reaction between quinolines **1** derivatives with toluene **24** under visible light irradiation (Scheme 11).[19] Initial investigations were carried out on *p*-xylene and 4-methylquinoline as model substrates for this Minisci-type CDC reaction. Optimized conditions revealed that light irradiation, photocatalyst, and bromide source are crucial for the transformation of this reaction. Out of various bromide additives screened, NH$_4$Br as a bromide source displayed the highest efficiency in reaction yield. A library of substituted quinoline derivatives **1** with electron-donating and withdrawing functionalities reacted well with toluene under the optimized conditions to afford the desired products **25** in 26-82% yield. Notably, toluene derivatives **24** bearing electron-donating groups gave higher product yield in comparison to those with electron-donating ones. Besides, ethylbenzene and 2-methylnapthlene also worked well to afford the desired product in 33-45% yield. A radical trapping experiment with TEMPO and 1,1-diphenylethylene supported the involvement of a radical mechanistic pathway. Quantum yield experiment (Φ = 0.52), eliminated the possibility of radical chain pathway. As shown in Scheme 11, the photoexcited catalyst undergoes SET with the bromide anion to form a bromine radical, which undergoes HAT with the toluene **24** to form a benzyl radical intermediate **11A**. This intermediate adds to the quinoline **1** to form an *N*-centered radical intermediate **11B**. Subsequently, the oxidized catalyst Ir(II) is reduced by the oxygen (O$_2$) to form a superoxide radical (HO$_2$·) along
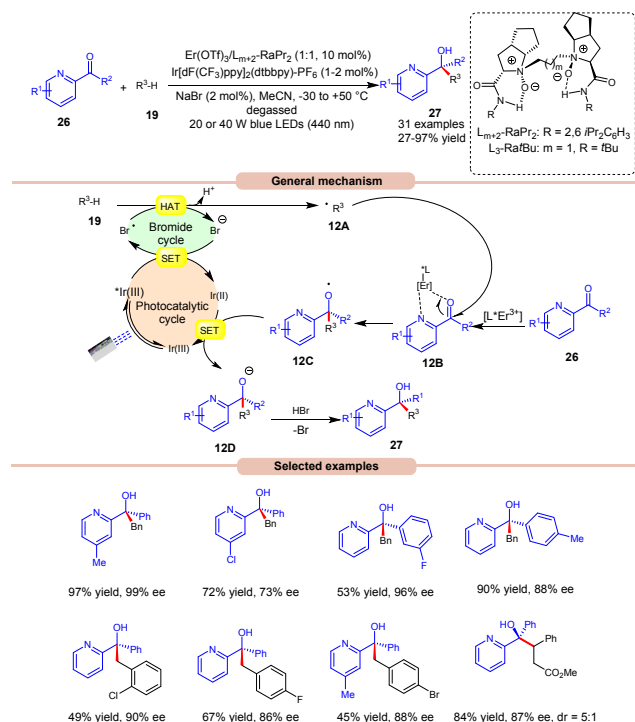
Scheme 12. Bromine radical enhanced photoreduction of ketones and hydrocarbons for synthesizing tertiary alcohols.

Scheme 13. Ir-catalyzed benzylic C(sp3)–H functionalization of alkylarenes with trifluoromethyl ketones.

with the completion of the catalytic cycle. This superoxide radical ($HO_2\cdot$) oxidizes the radical intermediate **11B** to generate a cation intermediate **11C**, which finally upon deprotonation yields the desired product **25**. The compatibility of this strategy was further demonstrated in the late-stage functionalization of biologically active molecules.

The following year, Liu, Feng and co-workers reported a bromine radical-mediated enantioselective photoreduction of ketones **26** and hydrocarbons **19** for the synthesis of tertiary alcohols **27** (Scheme 12).[20] Both electron-rich and electron-withdrawing groups on pyridine-based ketones **26** were converted into tertiary alcohols in good yields. However, *ortho*-substituted diarylketones gave a lower yield than the *meta*- and *para*-substituted ones, probably due to steric hindrance. Moreover, allylic and saturated cyclic hydrocarbons gave the required products **27** in good yields and enantioselectivity. Mechanistically, it is proposed that the photoexcited *Ir(III) undergoes SET with the bromide ion generating the bromine radical along with Ir(II). This bromine radical participates in HAT with the benzylic C(sp3)–H partner **19**, producing an alkyl radical intermediate 12A. Next, the pyridine-based ketones 26 coordinate with the chiral Er(III)-complex to generate the complex 12B. Therefore, the complex 12B undergoes spatial-selective radical addition with the alkyl radical 12A, generating the chiral radical intermediate 12C. Lastly, the resulting radical intermediate 12C undergoes SET/protonation to access the desired tertiary alcohols 27 with bromide ion, which again initiates the catalytic cycle.

Recently, Deng and co-workers established a visible light-induced benzylic C(sp3)–H functionalization of petroleum-derived alkylarenes **24** with trifluoromethyl ketones **28** to give
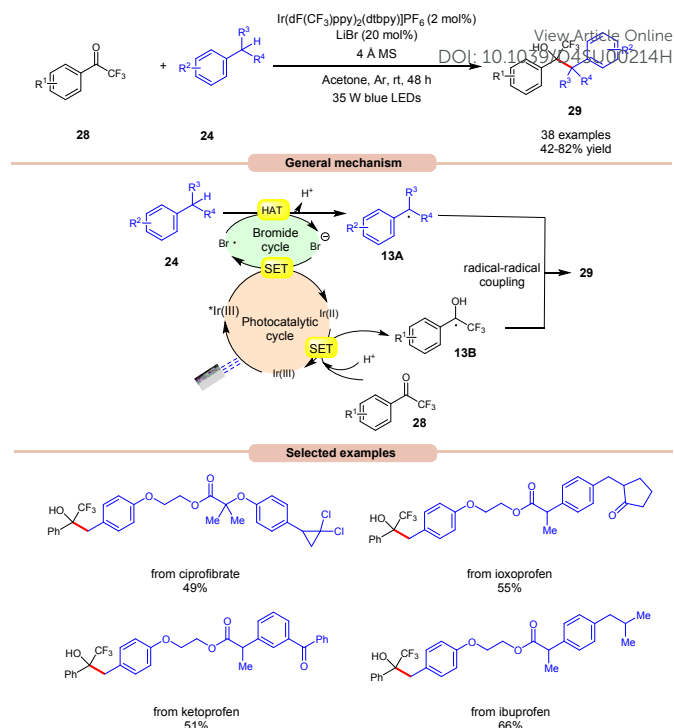
trifluoromethyl alcohols **29** (Scheme 13).[21] Substituted toluene **24** with electron-donating and electron-withdrawing groups at various positions were well tolerated, accessing the desired products **29** in 42-82% yields. Furthermore, the *meta*- and *ortho*-substituted toluene **24** gave the required products **29** in relatively low yields. In addition, methyl heteroarenes such as 2-thienyl, 2-furyl substrates, and 2-methylnaphthalene reacted smoothly and gave the corresponding products in moderate yields. The robustness of this protocol is further demonstrated by the late-stage functionalization of complex bioactive molecules such as isoxepac, ciprofibrate, ibuprofen, flurbiprofen, ketoprofen, and naproxen. Radical trapping experiments using TEMPO, BHT and hydroquinone suggest the involvement of a radical pathway. Mechanistically, photoexcited *Ir(III) complex oxidizes the bromine anion to generate the bromine radical, which abstracts a hydrogen atom alkylarenes **24** to give benzyl radical **13A**. Next, trifluoromethyl ketones **28** undergoes a proton-coupled electron transfer (PCET) process with the reducing Ir(II)-complex to give the ketyl intermediate **13B**. Finally, radical-radical coupling between the benzyl radical **13A** and ketyl intermediate **13B** affords the final desired product **29**.

In 2022, Huang, Deng and co-workers revealed a dual photoredox/nickel-catalyzed coupling of methyl arenes **24** with acid chlorides **30** *via* a bromine radical enhanced HAT pathway (Scheme 14).[22] The author utilized Ir-complex photocatalyst with $NiBr_2$ as a co-catalyst and bromine radical source in acetone. In this protocol, acid chloride **30** with electron-rich groups delivered better yields than the ones having electron-deficient groups.

ARTICLE
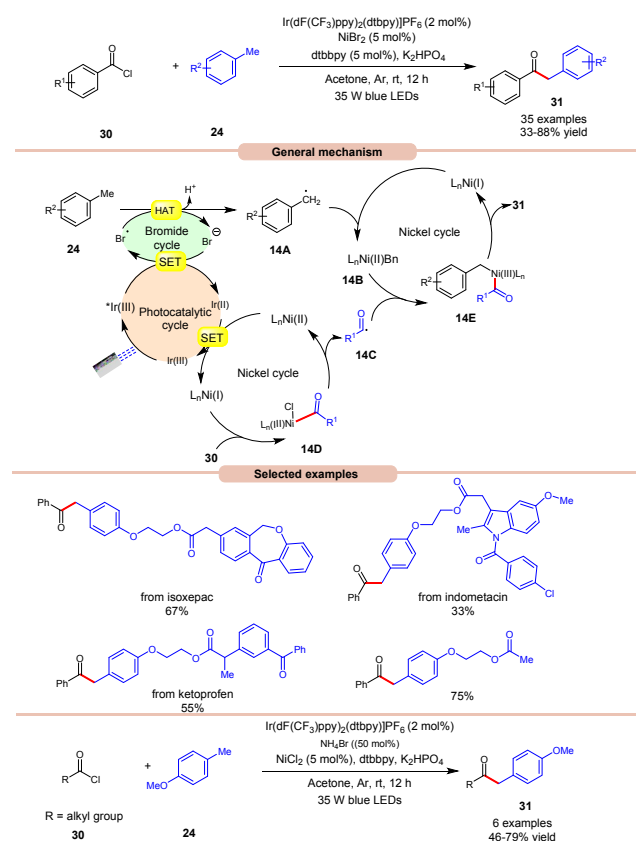
Scheme 14. Dual Ir/nickel-catalyzed coupling of methyl arenes with acid chlorides.

Unfortunately, 4-nitro benzoyl chloride did not work in this reaction. In the case of methylarenes, *para*-substituted derivatives displayed better reactivity compared to *meta*-, *ortho*-substituted due to steric hindrance. The compatibility of this method was demonstrated in the late-stage functionalities of complex drug molecules such as ioxoprofen, ketoprofen, and flurbiprofen, etc. Radical trapping experiments suggested the involvement of a radical pathway and their trapped adduct confirmed the formation of acyl radical. The authors proposed that reductive quenching of photoexcited *Ir(III) catalyst with bromine anion generates Ir(II) and bromine radical. Simultaneously, Ni(I) species were generated by the interaction between Ir(II) and Ni(II) species, which reacts with acid chlorides **30** to give acyl radical intermediate **14C** *via* intermediate **14D**. In turn, the methyl arene **24** undergoes HAT with the generated bromine radical to give radical intermediate **14A**, which upon oxidative addition with Ni(I) species generates Ni(II) intermediate **14B**. Lastly, the trapping of acyl radical **14C** and Ni(II) intermediate **14B**, followed by reductive elimination yields the final product **31**. With a change in reaction conditions, the authors demonstrated the utility of this method in the acylation of methyl arenes **24** using alkyl acid chlorides **30** in good yields.

In 2022, Deng and co-workers reported a dual Ir/Ni-catalyzed arylation of benzylic C-H bonds of toluene derivatives **24** with aryl bromides **32** (Scheme 15).[23] Here, cross-coupling reactions were successfully conducted with a wide range of aryl- and heteroaryl bromides **32** containing electron-deficient, neutral, or electron-donating functional groups. It was further observed that substrates
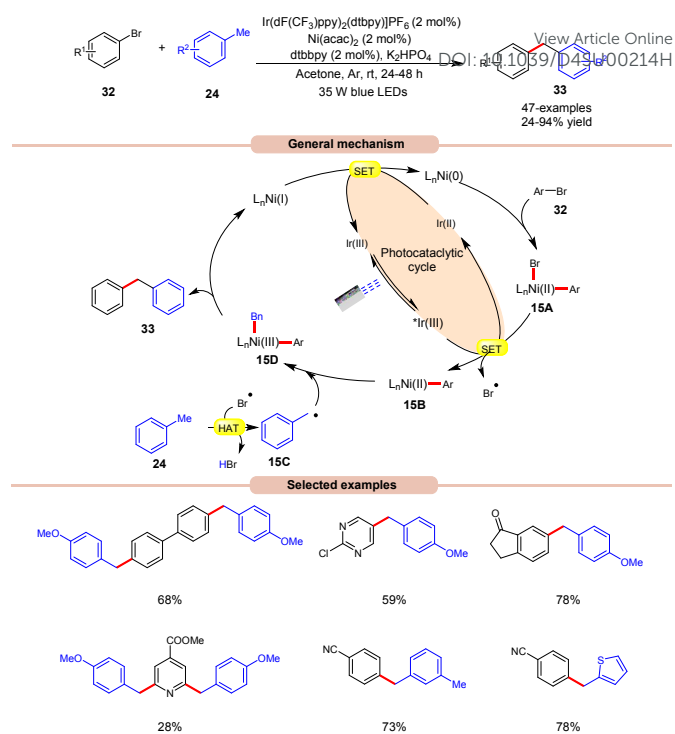

Scheme 15. Dual Ir/Ni-catalyzed arylation of benzylic C-H bonds of toluene derivatives with aryl bromides.

with electron-rich groups resulted in reduced yields of the corresponding coupling products **33**. Mechanistically, the Ni(II) aryl bromide intermediate **15A** was generated through the oxidative addition of Ni(0) complex to aryl bromide **32**. Next, the photoexcited *Ir(III) undergoes SET with **15A** to give an aryl Ni(II)-species **15B** and bromine radical (Br•). This bromine radical abstracts the hydrogen atom from toluene derivative **24**, to produce benzyl radical **15C**. Following this, the Ni(II) aryl species **15B** reacts with the benzylic radical **15C**, yielding the Ni(III) aryl alkyl species **15D**. Moreover, upon reductive elimination, the desired 1,1-diaryl alkanes **33** is formed with the generation of the Ni(I) species, which transforms into the Ni(0) species *via* SET with the Ir(II) complex, thus concluding both catalytic cycles. The synthetic versatility of this method was further demonstrated in the late-stage arylation or benzylation of numerous drug-like and complex molecules.
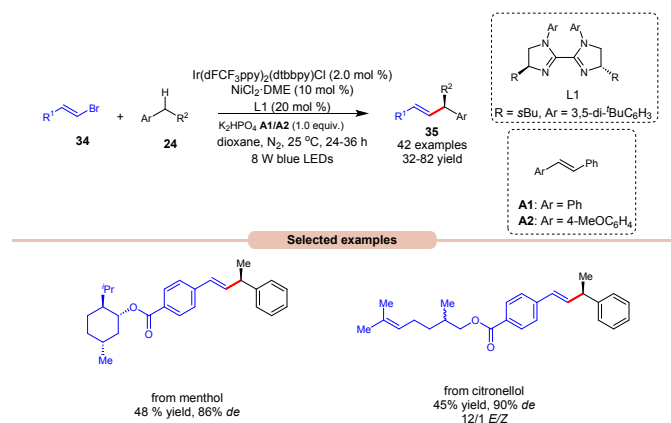
Scheme 16. Dual Ir/nickel-catalyzed synthesis towards stereo- and enantioselective benzylic C(sp3)-H alkenylation.
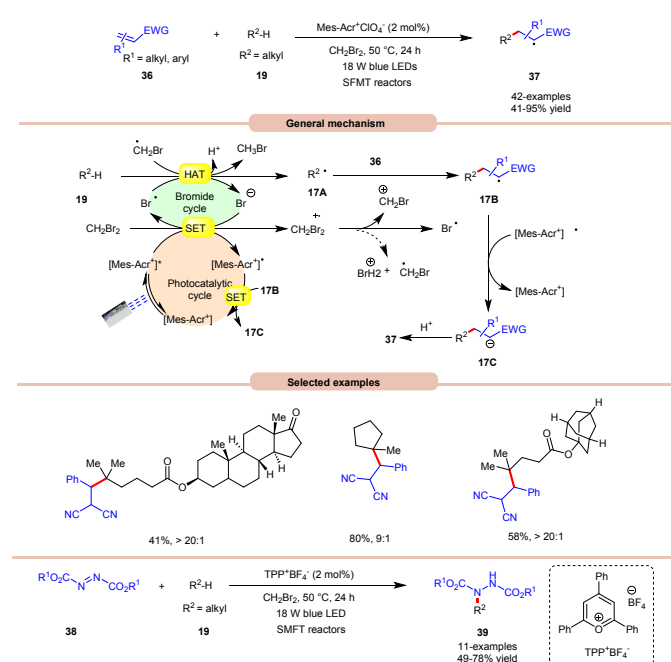
Scheme 17. Bromine radical-assisted alkylation and amination of C(sp3)-H bonds.

Alkenylation reactions are versatile tools in organic synthesis, enabling the formation of carbon-carbon double bonds with high efficiency and selectivity. They find wide applications in the preparation of pharmaceuticals, agrochemicals, and materials science.[24] In this context, Lu and coworkers demonstrated a stereo- and enantioselective benzylic C(sp3)-H alkenylation, using a dual Ir/nickel catalytic system towards the synthesis of chiral allylic compounds **35** (Scheme 16).[25] Easily accessible alkylbenzenes **24** and alkenyl bromides **34**, including complex molecules, participated in this cross-coupling reaction to afford the desired allylic compounds **35** in up to 93% ee and >20/1 E/Z ratio under mild reaction conditions with good functional group tolerance. Alkenyl bromides **34** with electron-rich or electron-deficient aryl substituents were well tolerated. It is crucial to underscore the significance of stilbene as an additive since it acts as a triplet energy transfer inhibitor. This function effectively blocks the direct energy transfer event from the

excited state photocatalyst to the product and eliminates the isomerization of the double bond. Furthermore, this methodology has been effectively utilized in bromides derived from natural products affording the desired products **35** in moderate yields. The mechanism for product formation occurs in the manner as discussed in previous Scheme 15.

An unprecedented approach towards the selective alkylation of unactivated C(sp3)-H bonds **19** was achieved by Wu and co-workers in 2020, using a stop-flow micro-tubing reactor (SFMT) under visible light irradiation (Scheme 17).[26] The authors observed that the utilization of CH_2Br_2 as a solvent, as well as a bromine radical source, was best suited for this alkylation reaction of tertiary unactivated C(sp3)-H **19** bond by using a metal-free acridinium catalyst (Mer-AcrClO$_4$). A series of tertiary alkanes **19** bearing electron-donating and electron-withdrawing alkyl and aryl groups reacted well affording the corresponding products **37** in 41-95% yields. This reaction was also achieved under higher reactivity when conducted under flow microtubing reactors, compared to batch reactors. Screening of different photocatalysts revealed that Mer-AcrClO$_4$ is highly reactive in catalyzing the reaction and bromine radical could be effectively generated from CH_2Br_2 under photocatalytic conditions. Mechanistically, the photoexcited catalyst oxidizes CH_2Br_2, which eventually gives a bromine radical. Furthermore, the tertiary alkyl group **19** undergoes HAT with bromine radical to give a radical intermediate **17A**. This intermediate interacts with the Michael acceptor **36** to give radical intermediate **17B**, accompanied by SET/protonation to yield the final product **37**. Moreover, this technology was also seen in the amination of C(sp3)-H bonds **19** using dialkyl azodicarboxylates **38** as an aminating reagent affording the corresponding products **39** in 49-78% yield. Notably, this method worked well with secondary and tertiary unactivated alkyl groups, whereas it failed with primary alkyl groups due to the lower stability of the alkyl radical.

4. Hydrogen atom transfer from α-heterocarbons

Hydrogen atom transfer (HAT) involving an α-heteroatom refers to the abstraction of a hydrogen atom bonded to a carbon atom adjacent to a heteroatom (such as nitrogen, oxygen, sulfur, etc.). This type of reaction commonly occurs in organic chemistry and plays a significant role in various chemical transformations. In a molecule containing α-heteroatom, the heteroatom can influence the reactivity of the adjacent carbon-hydrogen bonds. The electronegativity or the presence of lone pairs on the heteroatom can affect the bond strength and polarity of the adjacent C-H bond, making it more susceptible to abstraction by bromine radical (Br•).

ARTICLE   **Journal Name**
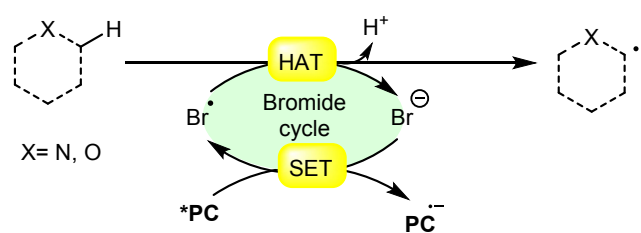
Scheme 18. General approach for α-heteroatom radical intermediate formation *via* bromine radical-mediated HAT.

In 2019, Huang and co-workers disclosed a visible light Ir-photoredox catalyzed Minisci-type alkylation of quinolines **1** with ethers **40** serving as the alkylating agents (Scheme 19).[27] The reaction demonstrates a wide range of functional group compatibility for both C2 and C4 couplings/alkylations of quinolines **1**. Notably, the C-4 substituted and unsubstituted quinolines, benzoquinolines provided the desired C-2 alkylated products **41** in 30-91% yields.
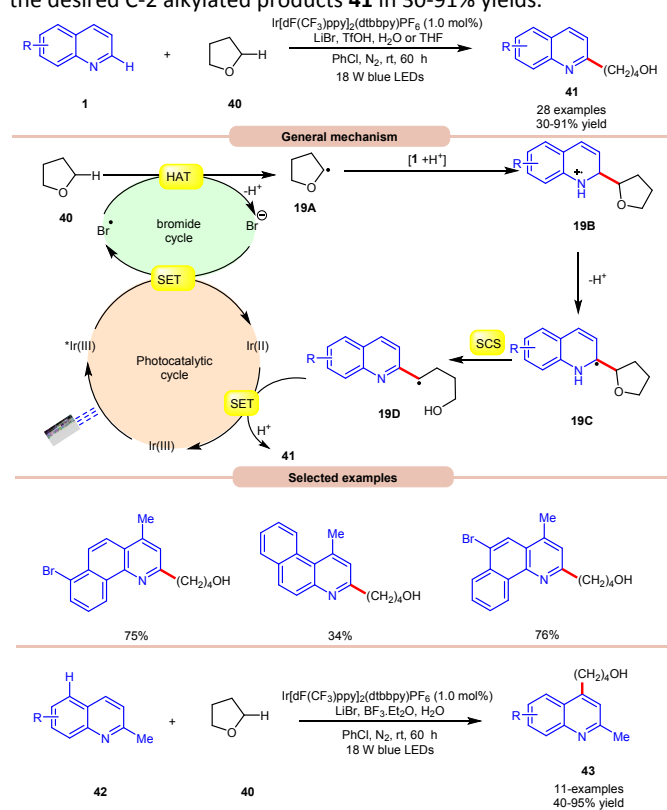
Scheme 19. Ir-photoredox catalyzed Minisci-type alkylation of quinolines with ethers.

Radical trapping experiment with TEMPO supports the involvement of a radical pathway. Mechanistically, the generated bromine radical (Br•) abstracts a hydrogen atom from THF **40**, resulting in the generation of an alkyl radical **19A**, which adds to the charged compound **1** leading to the formation of the radical cation **19B**. Subsequently, the radical cation **19B** undergoes deprotonation, followed by a spin-centre shift (SCS) process to ultimately give rise to an alkyl radical intermediate **19D** *via* C-O bond cleavage. Conclusively, SET/protonation of **19D**, ultimately yields the desired
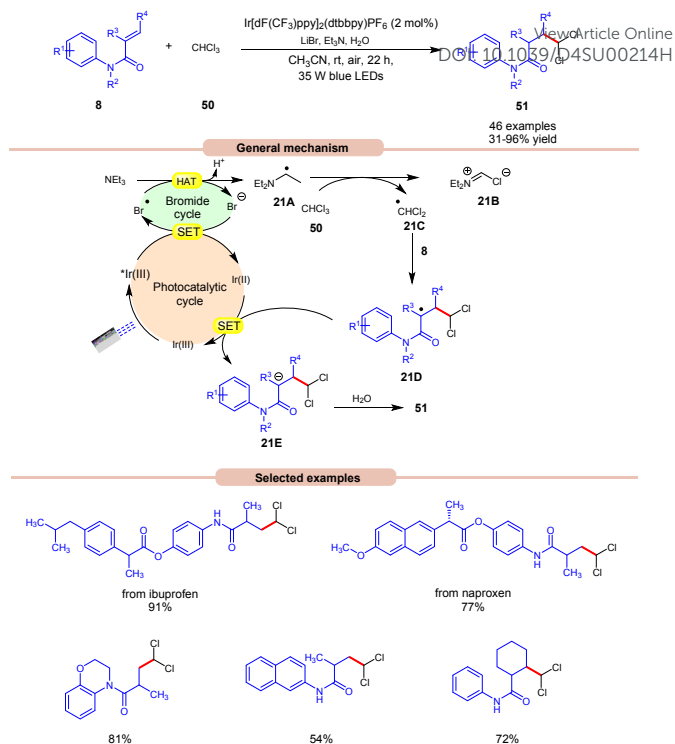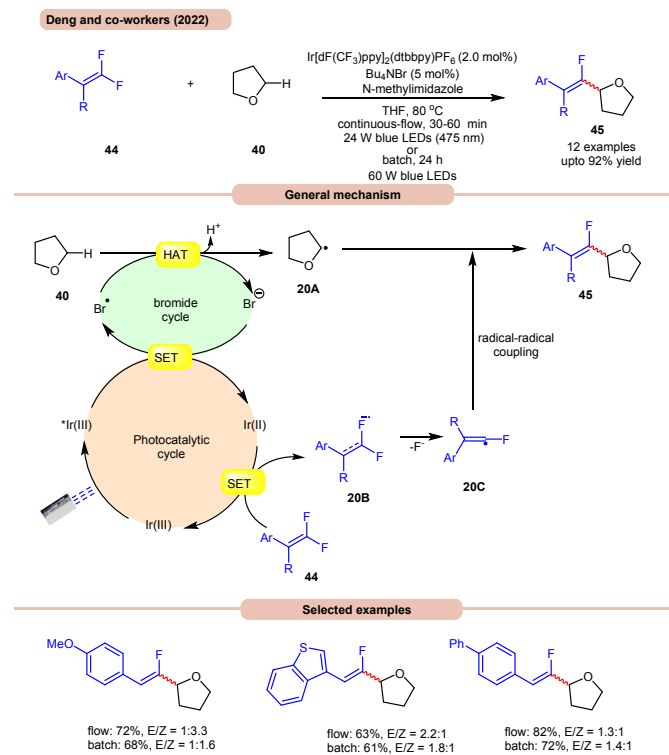
alkylated quinoline product **41**, while simultaneously regenerating the Ir(III) species.

In this work, an extension of C-2 blocked quinoline **42** gave the C-4 alkylated quinolines **43** in 40-95% yield by replacing TfOH with Lewis acid BF₃·Et₂O. The substrate scope revealed that 2-methylquinolines **42** with different functional groups were smoothly reacted to give the C-4 alkylated product **43**.

On the other hand, Deng and co-workers developed a visible-light Ir-photoredox catalyzed C(sp³)–H monofluoroalkenylation of ethers **40** for the synthesis of multi-substituted monofluoroalkenes **45** *via* selective HAT and radical-radical cross-coupling (Scheme 20a).[28a] This reaction shows high regioselectivity for the α-carbon atoms of THF **40** and thus allowing the synthesis of monofluoroalkenes **45** up to 92% yield. The substrate scope demonstrated a good functional group tolerance and could be carried out even on a gram scale.

Radical trapping experiments suggested that the reaction proceeds *via* a radical pathway. TEMPO-THF adduct was further confirmed by GCMS and 1,1-diphenylethylen-THF adduct was also isolated. As shown in Scheme 20, the key alkyl radical intermediate **20A** is formed *via* HAT between **40** and bromine radical. At the same time, the fluoroalkenyl radical **20C** was generated *via* SET reduction of **44** by Ir(II)-complex and cleavage of the C–F bond. Finally, targeted product **45** is generated by the radical-radical cross-coupling of **20A** and **20C**.

Deng and co-workers (2022)

Ir[dF(CF$_3$)ppy]$_2$(dtbbpy)PF$_6$ (2.0 mol%)
Bu$_4$NBr (5 mol%)
N-methylimidazole

THF, 80 °C
continuous-flow, 30-60 min
24 W blue LEDs (475 nm)
or
batch, 24 h
60 W blue LEDs

44 + **40** → **45**
12 examples
upto 92% yield

General mechanism

Selected examples

flow: 72%, E/Z = 1:3.3
batch: 68%, E/Z = 1:1.6

flow: 63%, E/Z = 2.2:1
batch: 61%, E/Z = 1.8:1

flow: 82%, E/Z = 1.3:1
batch: 72%, E/Z = 1.4:1

Ir[dF(CF$_3$)ppy]$_2$(dtbbpy)PF$_6$ (2.0 mol%)
Bu$_4$NBr (5 mol%)
NaHCO$_3$
60-80 °C, 24-48 h
24 W blue LEDs

44 + **19** → **46**
15-examples
44-97% yield

Huo and workers (2024)

Ir[dF(CF$_3$)ppy]$_2$(dtbbpy)PF$_6$ (1.0 mol%)
NaBr, Na$_3$PO$_4$
EtOAc, 20 °C, 24 h
40 W blue LEDs (427 nm)

47 + **48** → **49**
30 examples
21-92% yield

Selected examples

from diflunisal
75%

83%

74%

Scheme 20. Ir-photoredox catalyzed C(sp^3)–H monofluoroalkenylation of ethers.

Ir[dF(CF$_3$)ppy]$_2$(dtbbpy)PF$_6$ (2 mol%)
LiBr, Et$_3$N, H$_2$O
CH$_3$CN, rt, air, 22 h,
35 W blue LEDs

8 + CHCl$_3$ **50** → **51**
46 examples
31-96% yield

General mechanism

Selected examples

from ibuprofen
91%

from naproxen
77%

81%

54%

72%

Scheme 21. Dual Ir-photoredox/LiBr catalyzed 1,1-dichloromethylation of alkenes using chloroform.

The authors also illustrated the monofluoroalkenylation of cyclic and acyclic ethers, aliphatic aldehydes, and amides **19** as substrates, to afford the desired products **46** in 44-97% yields. It is worth noting that in Scheme 19, ring-opening of THF occurs, while in Scheme 20a, no ring-opening occurs in the reaction medium. This is due to the use of triflic acid (TfOH) in the reaction mixture, while in the absence of TfOH, no C-O cleavage occurs.

Huo and co-workers in 2024, reported a photoredox-catalyzed, bromine-radical-mediated C(sp3)– H difluoroallylation of amides **48** (Scheme 20b).[28b] The authors used Ir[dF(CF$_3$)ppy]$_2$(dtbbpy)PF$_6$ as a photocatalyst, NaBr as a HAT reagent, and Na$_3$PO$_4$ as a base in EtOAc under blue LEDs. This method incorporates both acyclic and cyclic-amino C(sp3)–H bonds **48** with a broad range of readily available trifluoromethyl alkenes **47**, providing difluoroallylated amine derivatives **49** with good to excellent yields.

Polychloromethylated hydrocarbons are omnipresent in various bioactive compounds and their synthesis have gained some attention in the scientific community.[29] In this regard, the synthesis of 1,1-dichloroalkane products **51** was achieved by Ji, Huang, and co-workers in 2022, using a dual Ir-photoredox/LiBr reaction system under visible light irradiation (Scheme 21).[30] Initial studies were carried out on *N*-phenylmethacrylamide **8** and chloroform **50** at room temperature. Out of various bases screened, the application of Et$_3$N was proven to be highly efficient, affording the desired product **51** in 31-96% yield with H$_2$O as a proton source and LiBr as an additive. *N*-phenylmethacrylamide **8** bearing various functional groups at the para-position of the benzene ring reacted well with chloroform **50**, affording the targeted products **51** in 62-96% yield.
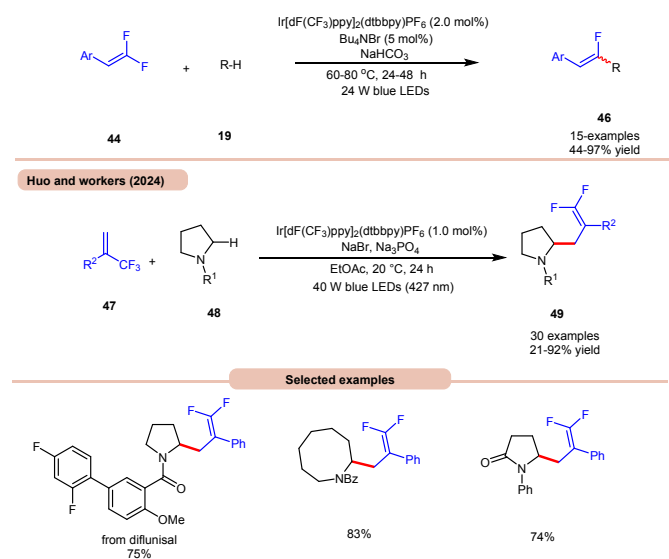
On the other hand, α-naphthyl and β-naphthyl substituted methylacrylamides **8** resulted in the targeted product in moderate yields (47-54% yield). Besides, *N*-phenylmethacrylamide **8** with internal and terminal alkenes smoothly reacted under the ideal conditions to yield the desired products in 39-86% yield. The compatibility of this reaction was further demonstrated in the late-stage functionalization of naproxen and ibuprofen derivatives resulting in the desired dichloromethylated products **51** in 77% and 91% yield, respectively. The generation of the •$CHCl_2$ radical intermediate is confirmed by a radical trapping experiment with 1,1-diphenylethylene. Deuterated studies with D_2O supported the incorporation of a proton source from H_2O to the α-position of the carbonyl group of the dichloromethylated product. As shown in Scheme 21, the photoexcited catalyst *Ir(III) oxidizes the bromide anion to a bromine radical intermediate, which participates in HAT with the Et_3N to give radical intermediate **21A**. This intermediate abstract a chlorine atom from $CHCl_3$ to give the key •$CHCl_2$ radical intermediate **21C**, which adds to the terminal alkene **8** to give radical intermediate **21D**. Finally, the desired product **51** is obtained *via* SET/protonation.

Giedyk and co-workers in 2020, disclosed a facile Ir-photoredox catalyzed Minisci-type alkylation of *N*-heteroarenes **1** with non-activated alkyl bromides **52** as radical precursors (Scheme 22).[31] This photochemical system has proven to be robust and versatile,

accommodating a wide range of primary and secondary alkyl bromides **52** with a variety of *N*-heterocycles **1**. Expectedly, secondary alkyl bromides **52** produced higher yields than that of primary ones, due to higher thermodynamic stability of the radical intermediate. Under the optimized conditions, the photocatalyst *Ir(III) oxidizes the bromide ion to generate bromine radical and Ir(II). This Ir(II) complex subsequentially absorbs a second photon, leading to the generation of a highly reducing state of the Ir complex *Ir(II). Next, the *Ir(II) complex undergoes a SET event with alkyl bromide **52** followed by fragmentation forming an alkyl radical **22A** and bromide anion, which participates in the catalytic cycle. The resulting alkyl radical **22A** adds to the *N*-heteroarenes **1**, followed by HAT with the bromine radical, which leads to the formation of the cation intermediate **22C**. Finally, the desired product **53** is obtained *via* work-up. Moreover, the authors demonstrated the C-H alkylation of heteroarene **1** by using cetyl trimethyl ammonium bromide (CTAB) as a cationic surfactant with NaBr in the reaction medium to give the desired product **53** in 39-92% yield. It is worth noting that, the reaction worked well with primary alkyls containing free hydroxy, chlorides, amides, and -CF_3 groups. Unfortunately, alkyl bromides bearing acetal group remained inactive under this protocol.

A visible light-mediated dual Ni/organophotoredox catalyzed C(sp³)–H cross-coupling reaction with aryl bromide **52** was disclosed by König and co-workers in 2020, using NaBr as a bromide source (Scheme 23).[32] A variety of linear and branched alkyl bromides **52** reacted well with the cyclic ether to afford the C(sp³)-H cross-coupling products **55** in moderate to good yields. Interestingly, benzyl chloride was also found to be an excellent coupling partner for this transformation. Moreover, the reaction could also be conducted on a gram scale. Based on previous reports, the authors postulated that the oxidative addition of Ni(0) into an aryl bromide **52** produces Ni(II) aryl bromide intermediate **23A**. Next, the photoexcited catalyst 4CzIPN* oxidizes **23A** to produce Ni(III) intermediate **23B**. Photolysis of **23B** results in the generation of a bromine radical and Ni(II) species **23C**. The resulting bromine radical rapidly abstracts a hydrogen atom from α-carbon to oxygen, resulting in a C-centered radical intermediate which adds to the Ni(II)-complex to produce Ni(III) species **23D**. Subsequently, reductive elimination yields the desired C(sp³)–H cross-coupling product **55**. Lastly, SET reduction of the resulting Ni(I) intermediate by the highly reducing 4-CzIPN•⁻ species regenerates the Ni(0)-complex, thus completing the catalytic cycle.
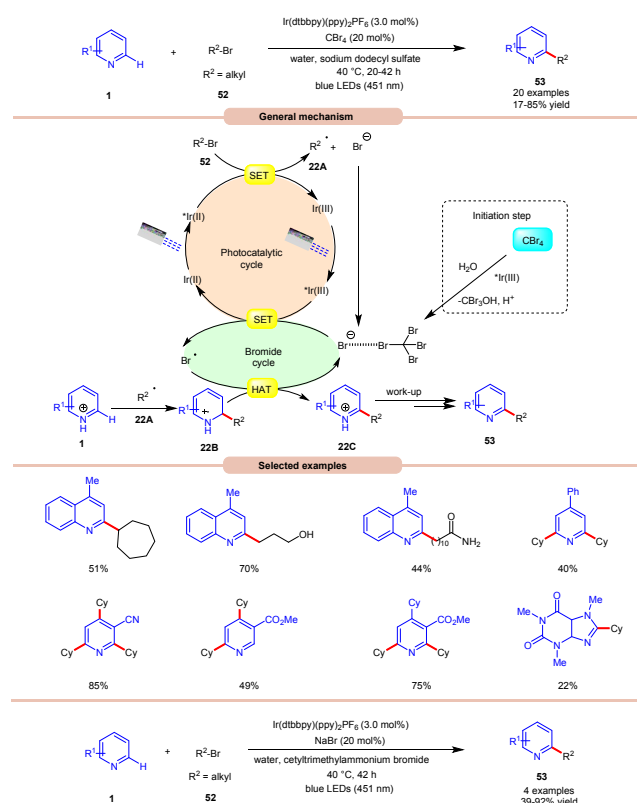

Scheme 22. Ir-photoredox catalyzed Minisci-type alkylation of *N*-heteroarenes with non-activated alkyl bromides.
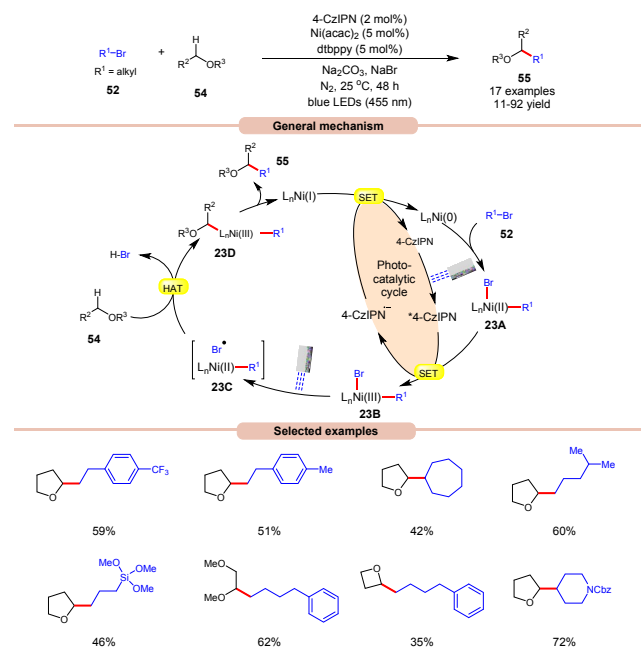
Scheme 23. Dual Ni/organophotoredox catalyzed C(sp³)–H cross-coupling reaction with aryl bromide.

In 2022, Song and co-workers reported a visible light-mediated direct C-H difluoroalkylation of quinoxalinones **56** with bromodifluoroacylarenes **57** via a C(sp³)–Br bond homolytic cleavage (Scheme 24a).[33a] In this method, quinoxalin-2(1H)-ones **56** bearing electron-rich or electron-deficient functionalities readily afforded the desired difluoroalkylated products **58** in 30-87% yields. Several control experiments were performed to determine the reaction mechanism. Under visible light irradiation, the C(sp3)–Br bond undergoes homolysis to generate a difluoroalkyl radical intermediate **24A**, which was further supposed by radical trapping experiments, and their adducts were confirmed by using HRMS analysis. Mechanistically, visible light-promoted C(sp3)–Br bond homolysis from ArCOCF₂Br **57** generated the difluoroalkyl radical intermediate **24A** and bromine radical. The bromine radical abstracts the hydrogen atom from quinoxalinone **56** to produce radical intermediate **24B** with the release of HBr. The generated radical intermediate **24B** undergoes radical coupling with difluoroalkyl radical **24A** to furnish the desired products **58**. The authors further expanded their work for the C(sp²)–H functionalization of aldehyde-derived hydrazones **59** with bromodifluoroacylarenes **57** for the direct preparation of functionalized α-iminodifluoroalkylated products **60**. The substrate scope revealed that a variety of (hetero)aryl aldehyde-derived hydrazones **59** bearing either electron-rich or electron-deficient groups were efficiently transformed into the required products **60** with good to excellent yields. In this protocol, unsaturated aldehydes-derived hydrazones **59** such as alkynals, alkenals, and ester aldehydes were also compatible to obtain a series of complex difluoroalkylated products **60**.
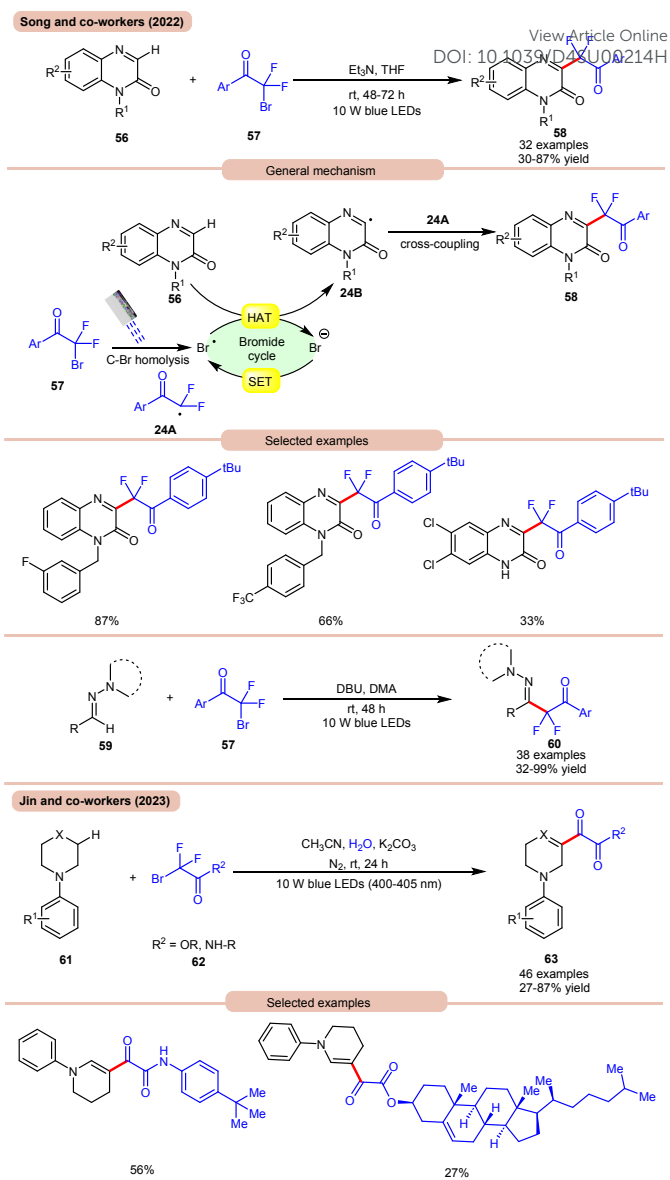
Scheme 24. Visible light mediated direct C-H difluoroalkylation of quinoxalinones with bromodifluoroacylarenes.

On the other hand, using difluoromethyl bromide **62** and H₂O, Jin and co-workers in 2023 reported the β-alkoxyoxalylation of N-aryl cyclic amines **61** for the synthesis of β-ketoester/ketoamides substituted enamines **63** in 27-87% yields (Scheme 24b).[33b] It was proposed that difluoromethyl bromide undergoes homolysis to give bromine radical, which participates in HAT and gives key difluoroalkylated intermediate. This intermediate further reacts in the presence of H₂O to give the desired product **63**. In 2021, Huang and co-workers disclosed a visible light-mediated photoredox Minisci alkylation reaction of 4-hydroxyquinazolines **65** with ethyl acetate **64** (Scheme 25).[34] In this protocol, 4-hydroxyquinazolines **65** bearing various electron-donating and electron-withdrawing functionalities reacted well with ethyl acetate **64** to afford the desired products **66**.
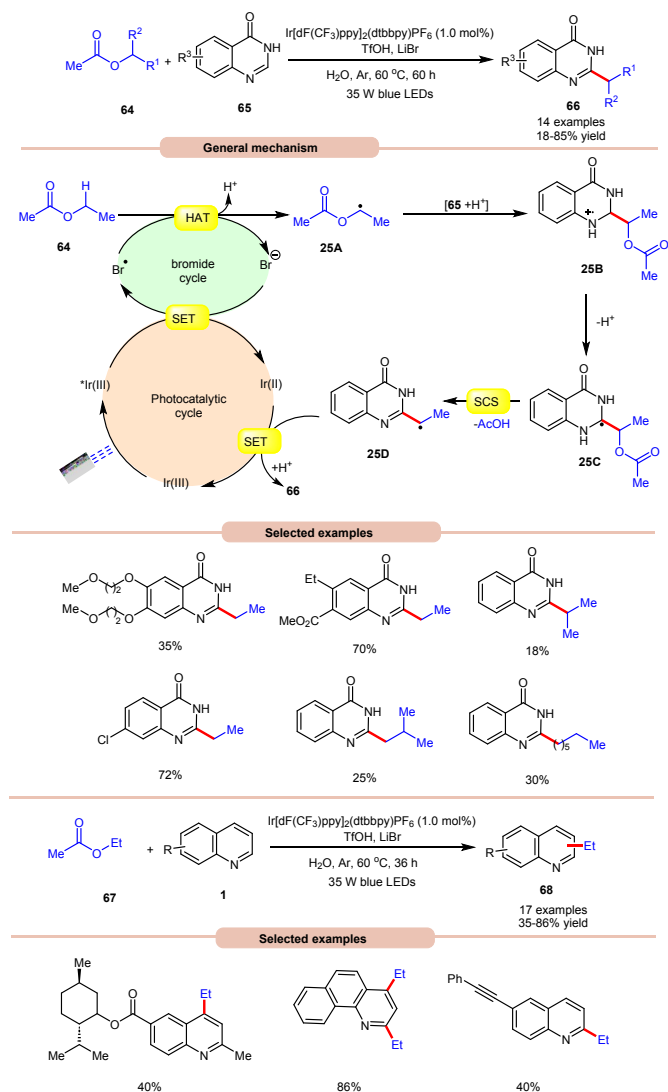
Scheme 25. Ir-catalyzed Minisci alkylation reaction of 4-hydroxyquinazolines with ethyl acetate.

Other alkylating reagents **64** such as isobutyl acetate, isopropyl acetate, *n*-pentyl acetate, *n*-butyl acetate, and *n*-heptyl acetate were also well tolerated affording the required product **66** in low to moderate yields (18-55%). The reaction was completely suppressed in the presence of TEMPO, BHT, and DPE, which supported the involvement of a radical mechanistic pathway. Mechanistically, the photoexcited catalyst *Ir(III) is reduced by the bromide ion, leading to the generation of a bromine radical (Br•). The bromine radical then initiates the abstraction of a hydrogen atom from ethyl acetate **64**, resulting in the formation of an alkyl radical **25A**. This alkyl radical **25A** undergoes a radical addition reaction with 4-hydroxyquinazoline **65**, accompanied by deprotonation leading to the formation of radical intermediate **25C**. Following this, a spin-center shift (SCS) process takes place, with the elimination of acetic acid (AcOH), resulting in the production of the radical intermediate **25D**. Finally, upon SET/protonation, the required alkylated product **66** is obtained. Simultaneously, this step regenerates the Ir(III) species, completing

the catalytic cycle. The applicability of this method was further demonstrated in the alkylation of quinolines and pyridines **1**
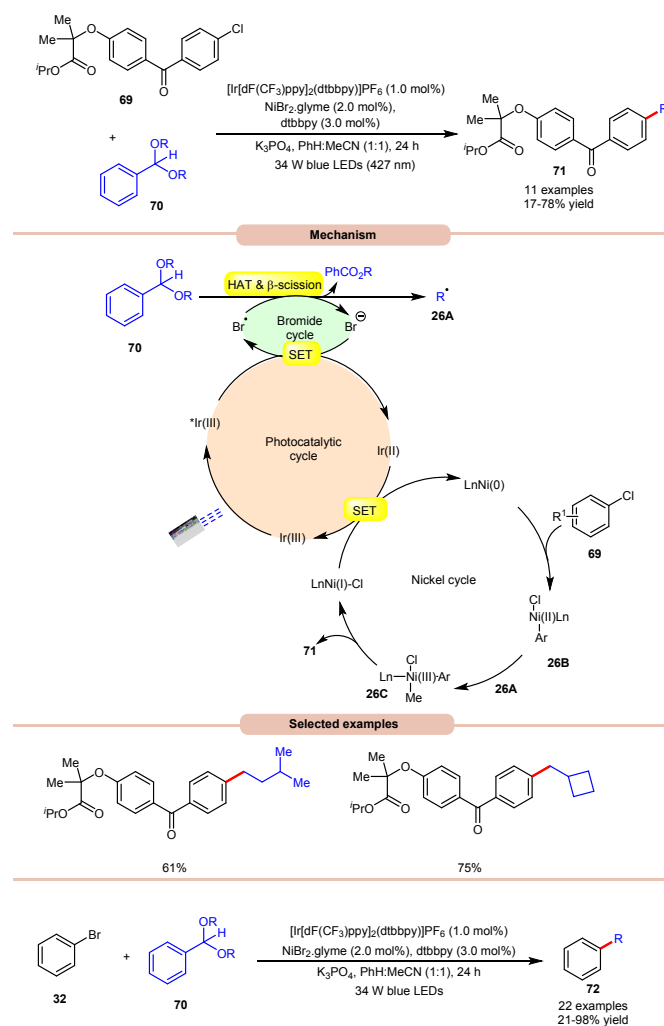
Scheme 26. Dual Ir/Ni-photoredox-catalyzed alkylation and (deutero)methylation of aryl halides.

derivatives under the optimized conditions giving the required product **68** in 35-86% yield.

Doyle and co-workers in 2022, reported a dual Ir/Ni-photoredox catalyzed alkylation and (deutero)methylation of aryl halides **69** by using benzaldehyde di(alkyl) acetals **70** (Scheme 26).[35] This protocol was found compatible with the late-stage functionalization of fenofibrate, which possesses an aryl chloride. The authors proposed that the photoexcited *Ir(III) oxidizes the bromide ion to a bromine radical, which undergoes HAT with the tertiary C–H bond of the acetal **70**, followed by β-scission to afford an alkyl radical **26A** and alkyl benzoate. Thereafter, Ni(0)-complex undergoes oxidative addition with an aryl chloride and produces a Ni(II) aryl chloride intermediate **26B**. The alkyl radical **26A** is captured by **26B**, generating Ni(III)-(Ar)(Me) species **26C**, accompanied by reductive elimination to yield the desired product **71** and Ni(I)-complex. The reduced photocatalyst Ir(II) can then reduce Ni(I) to regenerate both the Ir(III) and Ni(0)-catalysts. The authors further demonstrated the

C(sp²)–C(sp³) cross-coupling reaction between acetals **70** as sources of aliphatic coupling partners with aryl bromides **32** to give the desired products **72** in 21-98% yield.

5. Hydrogen atom transfer from (Me₃Si)₃SiH

Hydrogen atom transfer (HAT) from (Me₃Si)₃SiH (trimethylsilyl hydride) by a bromine radical is a well-known reaction in radical chemistry. Trimethylsilyl hydride is commonly used as a hydrogen atom donor in radical reactions due to its relatively weak Si-H bond and its ability to efficiently transfer a hydrogen atom to radical species. When a bromine radical encounters trimethylsilyl hydride, it can abstract a hydrogen atom from the Si-H bond, leading to the formation of a trimethylsilyl radical (Me₃Si)₃Si•) and hydrogen bromide (HBr). This process can be represented by the following equation:
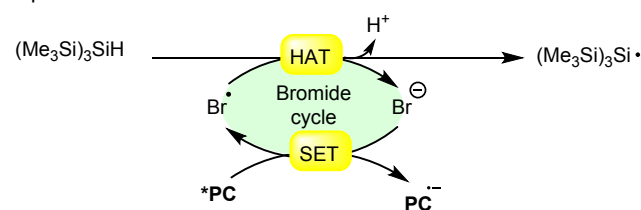

Scheme 27. General approach for trimethylsilyl radical intermediate formation *via* bromine radical-mediated HAT.

The resulting trimethylsilyl radical can further participate in various radical reactions, such as radical chain reactions or radical-mediated functionalization reactions. This type of hydrogen atom transfer is widely utilized in organic synthesis for the generation of radicals and the construction of complex molecules.
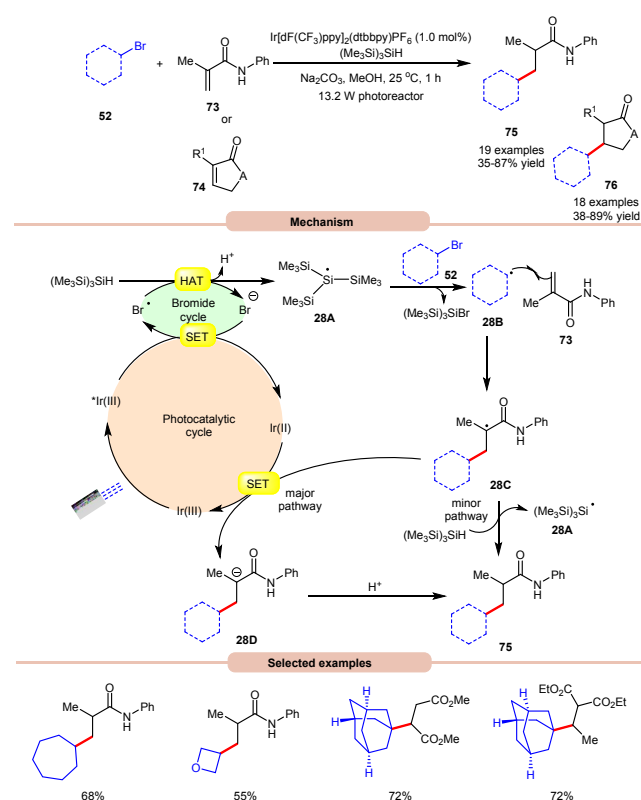
Scheme 28. Visible light-mediated Giese addition of unactivated alkyl bromides to electron-poor olefins.

In 2018, ElMarrouni, Balsells and co-workers introduced a mild procedure for the direct visible light-initiated Giese addition of unactivated alkyl bromides **52** to electron-poor olefins (Michael acceptor) **73** or **74** (Scheme 28).[36] In this process, visible light prompts the generation of an alkyl radical as a crucial intermediate from unactivated alkyl halides. This C(sp³)–C(sp³) bond formation proved to be highly efficient, accommodating a range of alkyl bromides were successfully applied in the reaction of cyclic or acyclic α,β-unsaturated esters and amides. Mechanistic investigations suggested that the photoexcited *Ir(III) complex oxidizes the bromide ion to form bromine radical, which abstracts a hydrogen atom from (Me₃Si)₃SiH to generate stabilized silyl radical intermediate **28A**. This intermediate **28A** rapidly undergoes halogen atom abstraction with the alkyl bromide **52**, giving rise to the alkyl radical **28B** and bromosilane by-product. The alkyl radical **28B** adds to the double bond of the Michael acceptor **73** generating another carbon radical intermediate **28C**. A single-electron transfer (SET) between radical intermediate **28C** and the reductant species Ir(II) provides an anion intermediate **28D**, which upon protonation furnishes the desired product **75**. Alternatively, hydrogen atom abstraction from (Me₃Si)₃SiH yields the corresponding product **75**, thereby regenerating stabilized silyl radical species **28A**. Notably, this methodology could be leveraged to access a key intermediate of vorinostat, an HDAC inhibitor employed in combating cancer and HIV.
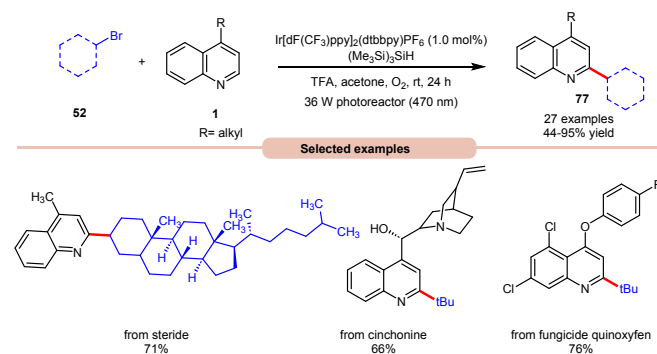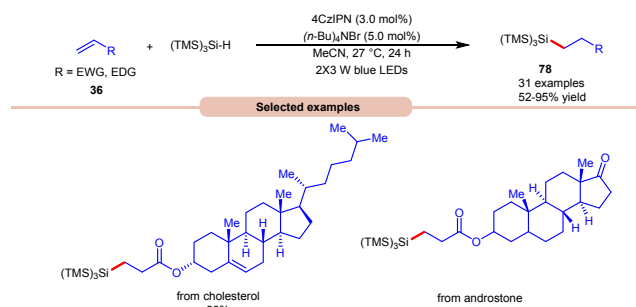

Scheme 29. Ir-photoredox catalyzed Minisci C–H alkylation of heteroarenes with unactivated alkyl halides.

In 2019, Wang and co-workers introduced a Ir-photoredox catalyzed Minisci C–H alkylation of heteroarenes **1** with unactivated primary, secondary, and tertiary alkyl bromides **52** by employing visible light irradiation (Scheme 29).[37] This method demonstrated the efficient incorporation of a diverse array of cyclic and acyclic, unactivated primary, secondary, and tertiary alkyl groups **52** into *N*-heteroarenes **1** under optimized reaction conditions. Impressively, the protocol exhibited scalability, successfully performing on a gram scale. Additionally, its robustness was demonstrated in the late-stage

ARTICLE

Journal Name

functionalization of complex *N*-containing natural products and drugs.

Scheme 30. Bromine radical-mediated hydrosilylation of alkene alkene using (TMS)$_3$SiH.

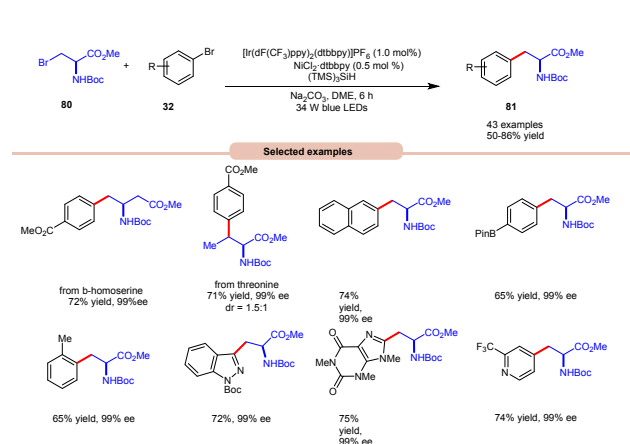Lately, Yu, Shihui, and co-workers revealed a bromine radical-mediated hydrosilylation of alkene **36** using (TMS)$_3$SiH and (*n*-Bu)$_4$NBr as a HAT reagent (Scheme 30).[38] A wide range of electron-deficient alkenes and electron-rich alkenes **36** reached under this protocol to give the desired hydrosilylated products **78** in moderate to excellent yields. The compatibility of this method was further demonstrated in the late-stage functionalization of bioactive molecules in good yields.

MacMillan and co-workers in 2016, developed a dual Ir/Ni-catalyzed approach towards the formation of C(sp3)–C(sp2) bond *via* cross-electrophile coupling between alkyl **52** and aryl bromides **32** in good

Scheme 31. Dual Ir/Ni-catalyzed approach towards the formation of C(sp3)–C(sp2) bond *via* cross-electrophile coupling between alkyl and aryl bromides.

Scheme 32. Dual Ir/Ni-catalyzed cross-electrophile coupling between alkyl halides and a diverse range of aryl halides.
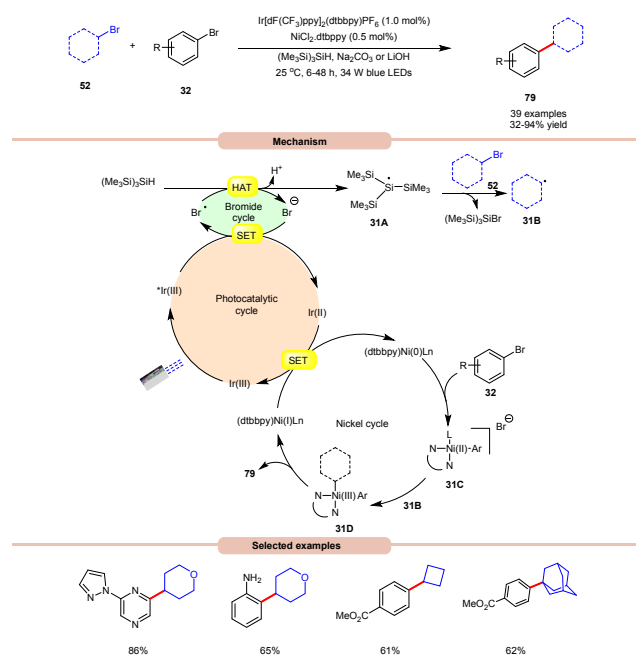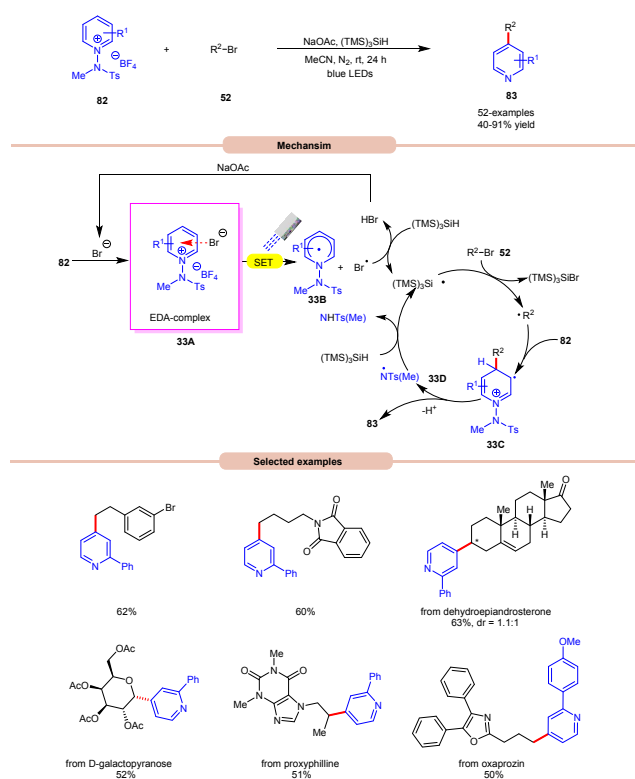
to excellent yields (Scheme 31).[39] The study of substrate scope showed that aryl bromide **32** featuring electron-rich and electron-deficient substituents, was compatible with the given reaction conditions. Interestingly, unprotected 2-bromo aniline substrate can be employed directly and give the corresponding product in 65% yield. Additionally, *N*-containing heterocycles such as pyrazine, pyrimidine, pyridazinequinolone, isoquinoline, and pyrazole-substituted pyrazine were well tolerated under the reaction conditions. Furthermore, cyclic and acyclic alkyl bromide **52** worked well. Mechanistically, the photoexcited *Ir(III)-complex oxidizes the bromide anion to generate bromine radical *via* the SET process, which upon HAT from tris(trimethysilyl)silane (TTMS) forms a stabilized silyl radical intermediate **31A**. Subsequently, silyl radical intermediate **31A** rapidly abstracts a halogen atom from the alkyl bromide **52** to form alkyl radical **31B** and the silyl bromide by-product. Moreover, a Ni(0)-complex undergoes oxidative addition with the aryl bromide **32** to form Ni(II)species **31C**, which then interacts with an alkyl radical **31B** to yield the Ni(III)-complex **31D**. Reductive elimination of **31D** delivers the desired C(sp3)–C(sp2) cross-coupling product **79** and a Ni(I) intermediate, which continues the catalytic cycle.

In the extension of their previous work, MacMillan and co-workers in 2021, disclosed a dual photoredox Ir/Ni-catalyzed cross-electrophile coupling between an alkyl halides **80** and a diverse range of aryl bromides **32** to produce artificial analogues of tryptophan, phenylalanine, and histidine derivatives (Scheme 32).[40] Various aryl bromides **32**, featuring electron-donating and electron-withdrawing groups were successfully utilized, leading to the desired products **81** in moderate to excellent yields.

Additionally, substitution at the *ortho*-, *meta*-, and *para*-positions was well-accommodated, albeit ortho-substituted aryl halides **32** necessitated a higher loading of the nickel catalyst (5 mol %). Hong and co-workers achieved the synthesis of C4-alkylated pyridines **83**

through an EDA-complex between pyridinium salts **82** and bromide ion under visible-light irradiation (Scheme 33).[41]

the desired C4-alkylated pyridine product **83**, regeneration of the silyl radical *via* *N*-centered radical intermediate **33D**, which propagates the chain.

**Scheme 33.** Bromide anion catalyzed the alkylation of pyridinium salt.

A wide range of primary, secondary, and tertiary alkyl bromides **52** efficiently participated under the optimized conditions, yielding the desired products **83** in 40-91% yield. Initial experiments with pyridinium salt and bromocyclohexane indicated that *in-situ* generated bromide anion effectively initiated a radical chain reaction under visible light irradiation, eliminating the need for an external bromide source. However, by employing tetrabutylammonium bromide (TBAB) as a bromide anion source resulted in reduced yields of the targeted product. UV-visible absorption studies confirmed the formation of an EDA complex between bromine anion and pyridinium salt **82**. Stern-Volmer experiments revealed the formation of bromine radical *via* reductive quenching of pyridinium salt **82** with the bromine anion. Moreover, the high quantum yield (Φ = 19.0) supported the involvement of a radical chain pathway. Mechanistically, an EDA-complex **33A** is formed between pyridinium salt (acceptor) **82** and bromide anion (donor). Visible light irradiation triggered a SET event, producing a bromine radical that initiated the chain reaction by abstracting an H-atom from (TMS)$_3$SiH. The resulting silyl radical captures the bromine atom from alkyl bromides **52** to generate the corresponding alkyl radical (R•). This alkyl radical regioselectively adds to the C4-position of the pyridinium salt **82**, followed by deprotonation and homolytic N-N bond cleavage to yield

6. Hydrogen atom transfer from allylic carbons

The allylic position is particularly reactive due to the stability of the resulting allylic radical, which is resonance-stabilized. Allylic hydrogen atom transfer can occur through radical reactions, where a bromine radical abstracts a hydrogen atom from the allylic carbon as shown in Scheme 34.
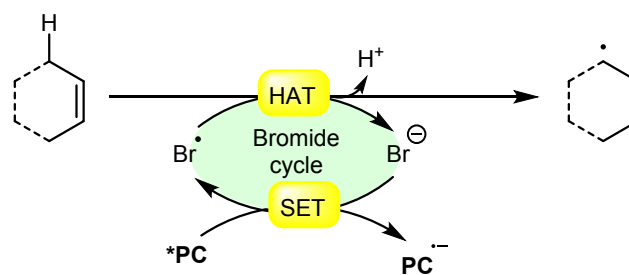
Scheme 34. General approach for allylic radical intermediate formation *via* bromine radical-mediated HAT.
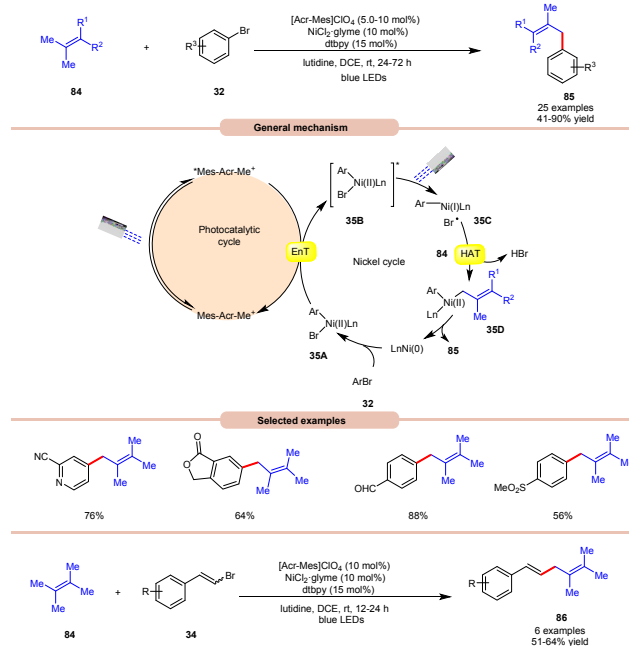
Scheme 35. Dual acridinium/Ni-catalyzed cross-coupling reaction between allylic compounds and aryl bromides.

The acridinium and Ni-catalyzed cross-coupling reaction between allylic compounds **84** and arylbromides **32** was reported by Rueping and coworkers in 2018 (Scheme 35).[42] Under the optimized reaction conditions, the oxidative addition of aryl bromide **32** to Ni(0) complex gives a Ni(II) complex **35A**. Next, the triplet–triplet energy

transfer (EnT) occurred from the photoexcited catalyst *Mes-Acr-Me$^+$ and Ni(II) complex **35A** to give intermediate **35B**. After that, The excited form of Ni(II) complex **35B** undergoes a homolytic bond cleavage of the Br–Ni bond and generates a bromine radical and a Ni(I) complex **35C**. The weak allylic C–H bond of alkene **84** undergoes H-atom transfer to the bromine atom and gives HBr and allylic radical

is formed in the reaction protocol and nBu$_4$NBr is important for product formation. Based on these studies, the authors proposed that the photoexcited catalyst *RB undergoes EnT process with O$_2$ to form s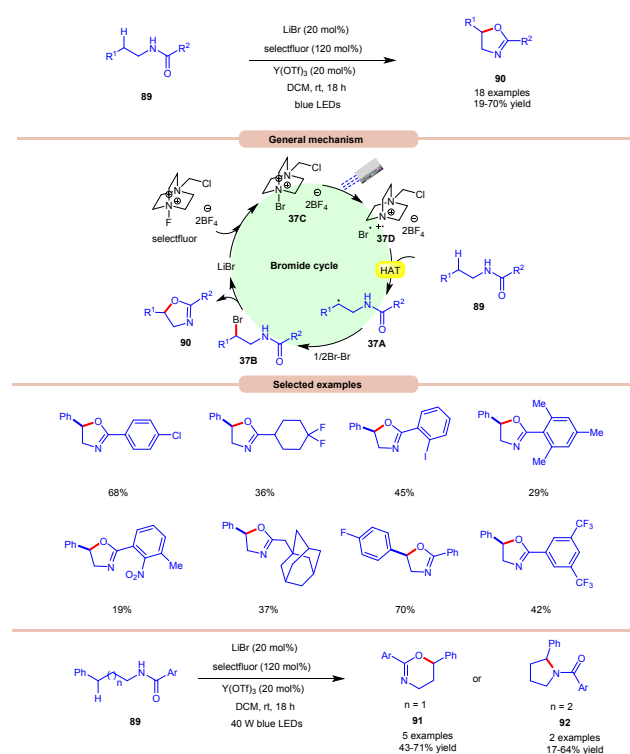inglet oxygen (^{1}O$_2$), which itself participates in SET with bromide anion to form bromine radical and superoxide radical intermediate. Thereafter, substrate **87** undergoes HAT with the bromine radical to form C-centered radical intermediate **36A**. This intermediate reacts with the superoxide radical to form an anion intermediate **36B**. Finally, upon protonation and elimination of H$_2$O give access to the final enone product **88**. This strategy offers a straightforward strategy for the allylic C-H oxidation of structurally challenging and complex molecules.

7. Miscellaneous

Scheme 36. Rose Bengal mediated allylic oxidation for the synthesis of enones.

35D. lastly, reductive elimination occurs to give the final product **85**. This reaction is also compatible with vinyl bromides **34** to yield the desired products **86** in 51-64% yield.

Thereafter, a novel and efficient approach towards the aerobic allylic C–H bond oxidation was achieved by Cai and co-workers in 2022 using nBu$_4$NBr as a bromide source, with Rose Bengal as a photocatalyst under visible light irradiation (Scheme 36).[43] This strategy was applicable to a wide range of tertiary cyclohexenols derivatives **87** as well as those containing 5, 7, 8 membered cyclic ring and acyclic derivatives, affording the desired enone products **88** in 33-91% yield. The robustness of this photocatalytic aerobic reaction was also found compatible with a wide range of pharmaceutically active steroids and triterpenes derivatives, resulting in the required products **88**. Detailed mechanistic studies were performed to gain insights about the reaction mechanism. Radical quenching with TEMPO and DABCO (singlet oxygen quencher) confirmed the involvement of singlet oxygen in the reaction protocol. Stern-Volmer experiments supported the higher quenching efficiency of molecular oxygen with Rose Bengal compared to other reactants. When performed in the absence of nBu$_4$NBr, the reaction resulted in the formation of the keto-acid product under similar conditions, indicating that the singlet oxygen

Scheme 37. Visible light-mediated bromine radical catalyzed synthesis of oxazolines, pyrrolidines, and dihydrooxazine.

Li and co-workers in 2021, demonstrated a bromide-catalyzed C–H functionalization of amide carbonyl carbon for the synthesis of oxazolines, pyrrolidines, and dihydrooxazine (Scheme 37).[44] For the synthesis of oxazolines, N-phenethylbenzamide derivatives **89** was employed as a standard substrate with LiBr as a bromide catalyst with F-TEDA-BF$_4$ (selectfluor) as an oxidant and Y(OTf)$_3$ as an additive under visible light irradiation. An array of electron-donating and withdrawing functionalities on the N-phenethylbenzamide derivatives **89** reacted smoothly to afford the desired product **90** in 19-70% yield. Notably, substrates bearing bulky arene groups such as 2,4,6-trimethyl or o-nitro or 3,5-CF$_3$ groups afforded the targeted products in diminished yields. Mechanistic studies reveal that visible light, selectfluor, and air were indispensable for the reaction. The generation of N-centered radical intermediate was ruled out from selectfluor (N–F bond homolysis) since no product bearing fluorine groups were observed. From these observations, the authors

ARTICLE

proposed the formation of intermediate **37C** by the interaction between LiBr and selectfluor, which in the presence of light generates *N*-centered cation radial intermediate **37D** *via* fragmentation. Next, the *N*-phenethylbenzamide derivatives **89** undergoes intermolecular HAT with the bromine radical to form C-centered radical intermediate **37A**. Next, upon bromination, accompanied by subsequent cyclization and deprotonation yields the desired oxazoline product **90** with the regeneration of the bromide catalyst. High loading of catalyst and additive was the only limitation of this method. The authors further demonstrated the synthesis of dihydroxazines **91** and pyrroline **92** under the reaction protocol.

8. Conclusions

This article provides an overview of C–H activation reactions initiated by Br• radicals generated through photocatalytic interactions with catalyst under visible light irradiation. These Br• radicals serve as appealing hydrogen atom transfer (HAT) reagents and electron acceptor due to their robust oxidative properties and the formation of strong covalent bonds with hydrogen atoms. Moreover, the efficient generation of Br• radicals *via* light irradiation offers advantages in terms of reaction control. Compared to conventional synthetic methods, it can offer a more efficient and resource-conserving approach to constructing complex organic compounds. Despite significant advancements made in this area, there are still many opportunities and challenges remaining, such as: (1) In this review article, the majority of the bromine radical mediated strategies are accelerated by expensive Ir-photoredox catalysis, sometimes in combination with nickel/ligand system. This leaves room to explore other inexpensive metal and non-metal catalysts for their successful execution and ease the pathway to generate bromine radical, which takes part in HAT reaction; (2) exploring of electron-donor-acceptor (EDA) complex strategies and strategies involving visible light-mediated homolysis without the need for a photocatalyst, in the generation of bromine radical is highly desirable; (3) Majorily, C-C, and C-O bond formations have been reported under these strategies, however, methods for the construction of C-N, C-S, C-P, C-X (X = halides) is still unexplored under bromine radical (Br•) mediated HAT strategies. We hope that this review will stimulate interest in C–H activation reactions involving bromine radicals (Br•) *via* HAT and deepen the understanding of their reactivity, thereby aiding in their application across various academic and industrial levels.

Conflicts of interest

The authors have no conflicts of interest.

Acknowledgements

References

1   (*a*) C. R. J. Stephenson, T. Yoon and D. W. C. Macmillan, in Visible light photocatalysis in organic chemistry, 2018, Wiley-VCH, German; (*b*) D. A. Nicewicz and D. W. C. MacMillan, *Science*, 2008, **322**, 77–80; (*c*) D. S. Hamilton and D. A. Nicewicz, *J. Am. Chem. Soc.*, 2012, **134**, 18577-18580; (*d*) L. Marzo, S. K. Pagire, O. Reiser and B. König, *Angew. Chem. Int. Ed.*, 2018, 57, 10034-10072; *Angew. Chem.*, 2018, **130**, 10188-10228; (*e*) D. Ravelli, S. Protti and M. Fognoni, *Chem. Rev.* 2016, **116**, 9850-9913; (*f*) X.-Y. Yu, J.-R. Chen and W.-J. Xiao, *Chem. Rev.* 2021, **121**, 506-561; (*g*) R. I. Patel, S. Sharma and A. Sharma, *Org. Chem. Front.*, 2021, **8**, 3166-3200; (*h*) N. Kvasovs, V. Gevorgyan, *Chem. Soc. Rev.*, 2020, **50**, 2244-2259; (*i*) K. L. Skubi, T. R. Blum and T. P. Yoon, *Chem. Rev.*, 2016, **116**, 10035-10074; (*j*) A. Y. Chan, I. B. Perry, N. B. Bissonnette, B. F. Buksh, G. A. Edwards, L. I. Frye, O. L. Garry, M. N. Lavagnino, B. X. Li, Y. Liang, E. Mao, A. Millet, J. V. Oakley, N. L. Reed, H. A. Sakai, C. P. Seath and D. W. C. MacMillan, *Chem. Rev.*, 2022, **122**, 1485-1542;   (*k*) T. Constantin, F. Julia and D. Leonori, *Chem. Rev.*, 2022, **122**, 2292-2352; (*l*) A. R. Allen, E. A. Noten and C. R J. Stephenson, *Chem. Rev.*, 2022, **122**, 2695-2751; (*m*) K. P. S. Cheung, S. Sarkar and V. Gevorgyan, *Chem. Rev.*, 2022, **122**, 1543-1625; (*n*) S. P. Pitre and L. E. Overman, *Chem. Rev.*, 2022, **122**, 1717-1751; (*o*) L. Chang, Q. An, L. Duan, K. Feng and Z. Zuo, *Chem. Rev.*, 2022, **122**, 2429-2486; (*p*) K. Kwon, R. T. Simons, M. Nandakumar, and J. L. Roizen, *Chem. Rev.* 2022, **122**, 2353-2428; (*q*) L. Capaldo, D. Ravelli and M. Fagnoni, *Chem. Rev.*, 2022, **122**, 1875-1924; (*r*) A. Tlili and S. Lakhdar, *Angew. Chem. Int. Ed.*, 2021, **60**, 19526-19549; (*s*) A. Tlili, and S. Lakhdar, *Angew. Chem. Int. Ed.*, 2021, **133**, 19678-19701; (*t*) R. I. Patel, J. Singh and A. Sharma, *ChemCatChem.*, 2022, **14**, e202200260; (*u*) B. Saxena, R. I. Patel, J. Tripathi and A. Sharma, *Org. Biomol. Chem.,* 2023, **21**, 4723-4743.

2   (*a*) C. K. Prier, D. A. Rankic and D. W. C. MacMillan, *Chem. Rev.*, 2013, **113**, 5322-5363; (*b*) T. Koike and M. Akita, *Inorg. Chem. Front.*, 2014, **1**, 562-576; (*c*) K. Teegardin, J. I. Day, J. Chan and J. Weaver, *Org. Process Res. Dev.*, 2016, **20**, 1156-1163; (*d*) D. A. Nicewicz and T. M. Nguyen, *ACS Catal.*, 2014, **4**, 355-360; (*e*) D. P. Hari and B. König, *Chem. Commun.*, 2014, **50**, 6688-6699; (*f*) M. H. Shaw, J. Twilton and D. W. C. MacMillan, *J. Org. Chem.*, 2016, **81**, 6898-6926; (*g*) C.-S. Wang, P. H. Dixneuf and J.-F. Soulé, *Chem. Rev.*, 2018, **118**, 7532-7585; (*h*) S. Sharma and A. Sharma, *Org. Biomol. Chem.*, 2019, **17**, 4384-4405; (*i*) W. M. Cheng and R. Shang, *ACS Catal.*, 2020, **10**, 9170-9196; (*j*) R. I. Patel, A. Sharma, S. Sharma and A. Sharma, *Org. Chem. Front.*, 2021, **8**, 1694-1718.

3   (*a*) C. G. S. Lima, T. D. M. Lima, M. Duarte, I. D. Jurbery and M. W. Paixão *ACS Catal.* 2016, **6**, 1389; (*b*) Y. Q. Yuan, S. Majumder, M. H. Yang and S. R. Guo, *Tetrahedron Lett.*, 2020, **61**, 151506; (*c*) P. Garra, J. P. Fouassier, S. Lakhdar, Y. Yagci, and J. Lalevée, *Prog. Polym. Sci.*, 2020, **107**, 101277; (d) G. E. M. Crisenza, D. Mazzarella and P. Melchiorre, *J. Am.Chem. Soc.* 2020, **142**, 5461 (*e*) B. Saxena, R. I. Patel and A. Sharma, *Adv. Synth. Catal.,* 2023, **365**, 1538-1564.

4   (*a*) L. Troian-Gautier, M. D. Turlington, S. A. M. Wehlin, A. B. Maurer, M. D. Brady, W. B. Swords and G. J. Meyer, *Chem. Rev.*, 2019, **119**, 7, 4628-4683; (*b*) S. Rohe, A. O. Morris, T. McCallum and L. Barriault, *Angew. Chem. Int. Ed.*, 2018, **57**, 15664-15669; (*c*) M. Zidan, A. O. Morris, T. McCallum and L. Barriault, *Eur. J. Org. Chem.*, 2020, **2020**, 1453-1458; (*d*) H. P. Deng, Q. Zhou and J. Wu, *Angew. Chem.*, 2018, **130**, 12843–12847.

5   (*a*) B. J. Shields and A. G. Doyle, *J. Am. Chem. Soc.* 2016, **138**, 12719-12722; (*b*) M. K. Nielsen, B. J. Shields, J. Liu, M. J. Williams, M. J. Zacuto and A. G. Doyle, *Angew. Chem. Int. Ed.*, 2017, **56**, 7191-7194; (*c*) S. K. Kariofillis, B. J. Shields, M. A. Tekle-Smith, M. J. Zacuto and A. G. Doyle, *J. Am. Chem. Soc.*,

RSC Sustainability Accepted Manuscript

2020, **142**, 7683-7689; (*d*) L. K. G. Ackerman, J. I. M. Alvarado and A. G. Doyle, *J. Am. Chem. Soc.*, 2018, **140**, 14059-14063; (*e*) Jin, Q. Zhang, L. Wang, X. Wang, C. Meng and C. Duan, *Green Chem.*, 2021, **23**, 6984-6989.

6 (*a*) J. M. Mayer, *Acc. Chem. Res.*, 2011, **44**, 1, 36-46; (*b*) L.-M. Zhao, Q.-Y. Meng, X.-B. Fan, C. Ye, X.-B. Li, B. Chen, V. Ramamurthy, C.-H. Tung and L.-Z. Wu, *Angew. Chem. Int. Ed.*, 2017, **56**, 3020-3024; (*c*) T. Ide, J. P. Barham, M. Fujita, Y. Kawato, H. Egami and Y. Hamashima, *Chem. Sci.*, 2018, **9**, 8453-8460; (*d*) E. L. Saux, M. Zanini and P. Melchiorre, *J. Am. Chem. Soc.*, 2022, **144**, 1113-1118; (*e*) T. Uchikura, K. Tsubono, Y. Hara, T. Akiyama, *J. Org. Chem.*, 2022, **87**, 15499-15510; (*f*) G. Kumar, S. Pradhan and I. Chatterjee, *Chem. Asian J.,* 2020, **15**, 651-672.

7 (*a*) H. P. Deng, X. Z. Fan, Z. H. Chen, Q. H. Xu and J. Wu, *J. Am. Chem. Soc.,* 2017, **139**, 13579–13584; (*b*) C. Y. Huang, J. Li, and C. J. Li, *Nat. Commun.* 2021, **12**, 4010.

8 (*a*) S. J. Blanksby and G. B. Ellison, *Acc. Chem. Res.*, 2003, **36**, 255-263; (*b*) Y. Shen, Y. Gu and R. Martin, *J. Am. Chem. Soc.* 2018, **140**, 12200-12209; (*c*) J. A. Kerr, Chem. Rev., 1966, **66**, 5, 465-500; (*d*) X.-S. Xue, P. Ji, B. Zhou and J.-P. Cheng, *Chem. Rev.*, 2017, **117**, 13, 8622-8648.

9 (*a*) L. Capaldo, L. L. Quadri and D. Ravelli, *Green Chem.*, 2020, **22**, 3376-3396; (*b*) L. Capaldo, D. Ravelli and M. Fagnoni, C*hem. Rev.,* 2022, **122**, 2, 1875–1924; (*c*) H. Cao, X. Tang, H. Tang, Y. Yuan and J. Wu, *Chem Catalysis,* 2021, **1**, 523–598; (*d*) H. Chena and S. Yu, *Org. Biomol. Chem.*, 2020, **18**, 4519-4532.

10 S. Bonciolini, T. Noël and L. Capaldo, *Eur. J. Org. Chem.*, 2022, e202200417.

11 Y. Itabashi, H. Asahara and K. Ohkubo, *Chem. Commun.*, 2023, **59**, 7506-7517.

12 Z. Wang, Q. Liu, X. Ji, G.-J. Deng, H. Huang, *ACS Catal.*, **2020**, **10**, 154-159.

13 X. Ji, Q. Liu, Z. Wang, P. Wang, G.-J. Deng and H. Huang, Green Chem., 2020, **22**, 8233-8237.

14 (*a*) K. Ding, Y. Lu, Z. Nikolovska-Coleska, G. Wang, S. Qiu, S. Shangary, W. Gao, D. Qin, J. Stuckey, K. Krajewski, P. P. Roller and S. Wang, *J. Med. Chem*. 2006, **49**, 3432-3435; (*b*) S. Peddibhotla, *Curr. Bioact. Compd.*, 2009, **5**, 20; (*c*) A. Millemaggi and R. J. K. Taylor, *Eur. J. Med. Chem.*, 2010, **2010**, 4527-4547; (*d*) M. Kaur, M. Singh, N. Chadha and O. Silakari, *Eur. J. Med. Chem.*, 2016, **123**, 858-894; (*e*) B. Yu, D.-Q. Yu and H.-M. Liu, *Eur. J. Med. Chem.*, 2015, **97**, 763-798; (*f*) N. Ye, H. Chen, E. A. Wold, P. Y. Shi and J. Zhou, *ACS Infect. Dis.*, 2016, **2**, 382–392.

15 Z. Sun, H. Huang, Q. Wang, C. Huang, G. Mao and G.-J. Deng, *Org. Chem. Front.*, 2022, **9**, 3506-3514.

16 (*a*) H. Wang, H. Liu, M. Wang, M. Huang, X. C. Shi, T. Wang, X. Cong, J. Yan and J. Wu, *iScience*, 2021, **24**, 6, 102693; (*b*) T. Ye, Y. Li, Y. Ma, S. Tan and F. Li, *J. Org. Chem.*, 2024, **89**, 534-540.

17 T. Kawasaki, N. Ishida and M. Murakami, *J. Am. Chem. Soc.*, 2020, **142**, 3366-3370.

18 (*a*) T. Kawasaki, N. Ishida and M. Murakami, *Angew. Chem. Int. Ed.*, 2020, **59**, 18267-18271; (*b*) T. Kawasaki, T. Tosaki, N. Ishida and M. Murakami, *Org. Lett.*, 2021, **23**, 7683-7687.

19 Q.-L. Wang, H. Huang, Z. Sun, Y. Chen and G.-J. Deng, *Green Chem.*, 2021, **23**, 7790-7795.

20 H. Yu, T. Zhan, Y. Zhou, L. Chen, X. Liu and X. Feng, *ACS Catal.*, 2022, **12**, 5136-5144.

21 Q.-L. Wang, H. Huang, M. Zhu, T. Xu, G. Mao and G.-J. Deng, *Org. Lett.*, 2023, **25**, 3800-3805.

22 Q.-L. Wang, H. Huang, G. Mao and G.-J. Deng, *Green Chem.*, 2022, **24**, 8324-8329.

23 Q.-L. Wang, Z. Sun, H. Huang, G. Mao and G.-J. Deng, *Green Chem.*, 2022, **24**, 3293-3299.

24 (*a*) M. B. Smith, J. March, March's Advanced Organic Chemistry: Reactions, Mechanisms, and Structure; John Wiley & Sons, Hoboken, NJ, 2013; (*b*) R. Álvarez, B. Vaz, H. Gronemeyer and A. R. de Lera, *Chem. Rev.*, 2014, **114**, 1-125; (*c*) M. Hassam, A. Taher, G. E. Arnott, I. R. Green and W. A. L. Van Otterlo, *Chem. Rev.*, **2015**, *115*, 5462-5569; (d) B. E. Maryanoff and A. B. Reitz, *Chem. Soc. Rev.*, *1989*, **89**, 863-927; (*e*) P. A. Byrne and D. G. Gilheany, *Chem. Soc. Rev.*, 2013, **42**, 6670-6696; (*f*) H.-T. Chang, T. T. Jayanth, C.-C. Wang and C.-H. Cheng, *J. Am. Chem. Soc.*, 2007, **129**, 12032-12041; (*g*) C. W. Cheung, F. E. Zhurkin and X. Hu, *J. Am. Chem. Soc.*, 2015, 137, 4932-4935; (*h*) B. Saxena, R. I. Patel, S. Sharma and A. Sharma, *Green Chem.*, 2024, **26**, 2721-2729; (*i*) Y. Ikeda, T. Nakamura, H. Yorimitsu and K. Oshima, *J. Am. Chem. Soc.*, 2002, **124**, 6514-6515; (*j*) W. Affo, H. Ohmiya, T. Fujioka, Y. Ikeda, T. Nakamura, H. Yorimitsu, K. Oshima, Y. Imamura, T. Mizuta and K. Miyoshi, *J. Am. Chem. Soc.*, 2006, **128**, 8068-8077; (*k*) K. Zhu, J. Dunne, M. P. Shaver and S. P. Thomas, *ACS Catal.*, 2017, **7**, 2353-2356; (*l*) S. J. Meek, R. V. O'Brien, J. Liaveria and R. R. Schrock, *Nature*, 2011, **471**, 461-466; (*m*) T. Di Franco, A. Epenoy and X. Hu, *Org. Lett.*, 2015, **17**, 4910-4913; (*n*) Q. Liu, X. Dong, J. Li, J. Xiao, Y. Dong and H. Liu, *ACS Catal.*, 2015, 5, 6111-6137.

25 X. Cheng, T. Li, Y. Liu, Z. Lu, *ACS Catal.* **2021**, *11*, 11059-11065.

26 P. Jia, Q. Li, W. C. Poh, H. Jiang, H. Liu, H. Deng and J. Wu, *Chem*, 2020, **6**, 1766-1776.

27 Z. Wang, X. Ji, T. Han, G.-J. Deng and H. Huang, *Adv. Synth. Catal.* **2019**, *361*, 5643-5647.

28 (*a*) C.-L. Cao, G.-X. Zhang, F. Xue and H.-P. Deng, *Org. Chem. Front.*, 2022, 9, 959-965; (*b*) Y. Lin, X. Shu and H. Huo, *Synthesis,* 2024, **56**, A-I.

29 (*a*) A. Butler, J. V. Walker, *Chem. Rev.*, 1993, **93**, 1937-1944; (*b*) D. Kahne, C. Leimkuhler, W. Lu and C. Walsh, *Chem. Rev.*, 2005, **105**, 425-448; (*c*) F. H. Vaillancourt, E. Yeh, D. A. Vosburg, S. Garneau-Tsodikova and C. T. Walsh, *Chem. Rev.*, 2006, **106**, 3364–3378; (*d*) C. Paul, G. Pohnert, *Nat. Prod. Rep.*, 2011, **28**, 186-195; (*e*) J. Latham, E. Brandenburger, S. A. Shepherd, B. R. K. Menon and J. Micklefield, *J. Chem. Rev.*, 2018, **118**, 232-269.

30 Y. Chen. Z. Qu, S. Chen, X. Ji, G-J. Deng and H. Huang, *Adv. Synth. Catal.*, 2022, **364**, 1573-1579.

31 M. S. Santos, M. Cybularczyk-Cecotka, B. König and M. Giedyk, *Chem. Eur. J.*, 2020, **26**, 15323–15329.

32 M. S. Santos, A. G. Corrêa, M. W. Paixão and B. König, *Adv. Synth. Catal.* 2020, **362**, 2367–2372.

33 (*a*) C.-H. Qu, R. Huang, Y. Liu, T. Liu, G.-T. Song, *Org. Chem. Front.*, 2022, **9**, 4135–4145; (*b*) B. Sun, P.-X. Li, Y. Jiang, L.-L. Yang, P.-Y. Huang, R.-P. Shen, M.-J. Chen, J.-Y. Wang and C. Jin, *Org. Lett.*, 2023, **25**, 6773–6778.

34 C. Wang, H. Shi, G.-J. Deng and H. Huang, *Org. Biomol. Chem.,* 2021, *19*, 9177–9181.

35 S. K. Kariofillis, S. Jiang, A. M. Żuranski,′ S. S. Gandhi, J. I. M. Alvarado and A. G. Doyle, *J. Am. Chem. Soc.*, 2022, **144**, 1045–1055.

36 A. ElMarrouni, C. B. Ritts and J. Balsells, *Chem. Sci.*, 2018, **9**, 6639-6646.

37 J. Dong, X. Lyu, Z. Wang, X. Wang, H. Song, Y. Liua and Q. Wang, *Chem. Sci.* 2019, **10**, 976–982.

38 Y. Zhao, K. Zhang, Y. Bai, Y. Zhang and S. Shi, *Chin. J. Org. Chem.*, 2023, **43**, 2837-2847.

Journal Name

39 P. Zhang, C. "Chip" Le and D. W. C. MacMillan, *J. Am. Chem. Soc.,* 2016, **138**, 26, 8084–8087.

40 T. M. Faraggi, C. Rouget-Virbel, J. A. Rincón, M. Barberis, C. Mateos, S. García-Cerrada, J. Agejas, O. de Frutos and D. W. C. MacMillan, *Org. Process Res. Dev*., 2021, **25**, 1966–1973.

41 S. Jung, S. Shin, S. Park and S. Hong, *J. Am. Chem. Soc*., 2020, **142**, 11370–11375.

42 L. Huang and M. Rueping, *Angew. Chem. Int. Ed*., 2018, **57**, 10333–10337.

43 C. Liu, H. Liu, X. Zheng, S. Chen, Q. Lai, C. Zheng, M. Huang, K. Cai, Z. Cai and S. Cai, *ACS Catal*., 2022, **12**, 1375–1381.

44 N. Kaur, E. C. Ziegelmeyer, O. N. Farinde, J. T. Truong, M. M. Huynh and Wei Li, *Chem. Commun*., 2021, **57**, 10387–10390.

RSC Sustainability Accepted Manuscript